THE LANCET
Planetary Health

Supplementary appendix

This appendix formed part of the original submission and has been peer reviewed. We post it as supplied by the authors.

Supplement to: Zhang S, Mwiberi S, Pickford R, et al. Longitudinal associations between ambient air pollution and insulin sensitivity: results from the KORA cohort study. *Lancet Planet Health* 2021; **5:** e39–49.

Appendix

Longitudinal associations between ambient air pollution and insulin sensitivity: results from the KORA cohort study

Siqi Zhang, MSc[1] Sarah Mwiberi, MSc[1,2] Regina Pickford, PhD[1] Susanne Breitner, PhD[1,3] Cornelia Huth, PhD[1,4] Prof. Wolfgang Koenig, MD [5,6,7] Prof. Wolfgang Rathmann, MD[4,8] Prof. Christian Herder, PhD[4,9,10] Prof. Michael Roden, MD[4,9,10] Josef Cyrys, PhD[1] Prof. Annette Peters, PhD[1,3,4,6] Kathrin Wolf, PhD[1,4*] and Alexandra Schneider, PhD[1,4*]

[1]Institute of Epidemiology, Helmholtz Zentrum München, German Research Center for Environmental Health, Neuherberg, Germany.

[2]Research Unit of Radiation Cytogenetics, Helmholtz Zentrum München, German Research Center for Environmental Health, Neuherberg, Germany.

[3]Institute for Medical Information Processing, Biometry and Epidemiology, Ludwig-Maximilians-Universität München, Munich, Germany.

[4]German Center for Diabetes Research (DZD), Munich-Neuherberg, Germany.

[5]German Heart Center Munich, Technical University of Munich, Munich, Germany.

[6]German Center for Cardiovascular Research (DZHK), Partner Site Munich, Munich, Germany.

[7]Institute of Epidemiology and Medical Biometry, University of Ulm, Ulm, Germany.

[8]Institute for Biometrics and Epidemiology, German Diabetes Center, Leibniz Center for Diabetes Research at Heinrich Heine University Düsseldorf, Düsseldorf, Germany.

[9]Institute for Clinical Diabetology, German Diabetes Center, Leibniz Center for Diabetes Research at Heinrich Heine University Düsseldorf, Düsseldorf, Germany.

[10]Division of Endocrinology and Diabetology, Medical Faculty, Heinrich Heine University, Düsseldorf, Germany.

[*]These authors made equal contributions and share last authorship.

Text S1. Definitions of individual characteristics

Body mass index (BMI) was calculated as weight divided by height squared. Occupational status was defined as employed if participants were employed, self-employed, or in training, and as unemployed/retired if participants were unemployed, homemakers, or retired. Educational attainment higher than secondary school was categorized as high, otherwise as low. Cumulative exposure to tobacco smoke (i.e. smoking pack-years) was assessed as the number of packs of cigarettes (20 cigarettes per pack) smoked per day multiplied by the years of smoking. Alcohol consumption was categorized into no (0 g/day), moderate (men 0·1–39·9 g/day and women 0·1–19·9 g/day), and high (men ≥ 40 g/day and women ≥ 20 g/day) consumption.[1] Physical activity was categorized based on the time spent on physical exercise into low (no or almost no physical exercise), medium (about one hour per week), and high (more than two hours per week) levels. Diabetes was defined as self-reported diabetes with confirmation by the respective physician or medical records and/or use of glucose-lowering medication (Anatomical Therapeutic Chemical code = A10), fasting glucose ≥ 126 mg/dl, or 2-h post glucose load glucose ≥ 200 mg/dl. Prediabetes included impaired glucose tolerance (defined as fasting glucose < 126 mg/dl and 2-h post glucose load 140 mg/dl ≤ glucose < 200 mg/dl) and impaired fasting glucose (defined as 110 mg/dl ≤ fasting glucose < 126 mg/dl). Normal glucose tolerance was defined as fasting glucose < 110 mg/dl and 2-h post glucose load glucose < 140 mg/dl.[2] Seasons of blood withdrawal were defined as spring: March-May; summer: June–August; autumn: September–November; winter: December–February.

Text S2. Measurement of biomarkers

Participants were asked to fast for at least eight hours before the visits to the KORA study center, during which time no food or liquid were allowed for intake except for mineral water. Physical exertion and smoking were also to be avoided on the day before and the morning before blood sampling. After a rest for 5–10 min, blood samples were collected in a sitting position.

Serum fasting insulin concentrations were measured by a microparticle enzyme immunoassay (Abbott, Wiesbaden, Germany) in S4, by an electrochemiluminescence immunoassay on a Cobas e602 instrument (Roche Diagnostics GmbH, Mannheim, Germany) in F4, and by a solid-phase enzyme-labeled chemiluminescent immunometric assay on an Immulite 2000 systems analyzer (Siemens) or by an electrochemiluminescence immunoassay on a Cobas e602 instrument (Roche) in FF4.[3,4] Serum fasting glucose concentrations were assessed by a hexokinase method (Gluco-quant, Roche) in S4, by a hexokinase method on a Dimension RxL (GLU Flex, Dade Behring, Deerfield, IL, USA) in F4, and by an enzymatic, colorimetric method using the GLU assay on a Dimension Vista 1500 instrument (Siemens) or using the GLUC3 assay on a Cobas c702 instrument (Roche) in FF4.[3,4]

The measurement instruments and assays of fasting insulin and glucose changed in KORA FF4 from Siemens to Roche halfway during the study. Calibration formulas were developed using 194 (122 for fasting glucose) FF4-samples measured with both methods during the time of the change. The Siemens fasting insulin results were calibrated to the Roche measurements using the following formula: Insulin_Roche = 1·307 µIU/mL + Insulin_Siemens × 1·016. No calibration was needed for fasting glucose because the double measurements were very similar, so that the intercept and the slope of the Passing-Bablok regression used for calibration were estimated to be zero and one, respectively. The distribution of fasting insulin concentrations among participants of the same age range was consistent across KORA S4, F4, and FF4, except that the 90th percentile of fasting insulin in S4 was higher than that in F4 and FF4, which might be due to a higher proportion of undiagnosed or untreated diabetic participants in S4. Thus, to make the fasting insulin and corresponding HOMA-IR and HOMA-B levels more comparable across three examinations, we excluded the observations with fasting insulin levels higher than the 90th percentile in S4 in a sensitivity analysis.

Text S3. Exposure assessment

Noise

We calculated the annual average day-night sound level four meters above the ground using a model developed by ACCON GmbH (Greifenberg, Germany).[5] This three-dimensional ground model considered all breaking edges, bridge constructions, and noise abatement walls at public roads, and took into account ground plan, occupancy, height, and reflection characters of around 87,000 buildings. Roads width, type, surface, traffic volume were used to describe roads in a network containing an overall length of 750 km in 2009.

NDVI (Normalized Difference Vegetation Index)

NDVI was derived from Landsat 5 Thematic Mapper satellite images captured in June 2000 (S4), 2007 (F4), and 2013 (FF4) at a spatial resolution of 30 m.[6] NDVI is calculated based on the difference of surface reflectance in visible (0·4–0·7 µm) and near-infrared (0·7–1·1 µm) wavelengths. NDVI values range from -1 to 1. Values close to one indicate a high density of green vegetation and values close to zero indicate barren areas of rock or sand. Negative values refer to blue spaces (water). In our study, we set all negative values to zero.

Back-extrapolated air pollutant concentrations

In the city of Augsburg, daily monitoring of background air pollution by routine continuous monitoring sites has been in operation since 1984. A map of the monitoring sites is shown in the figure below.

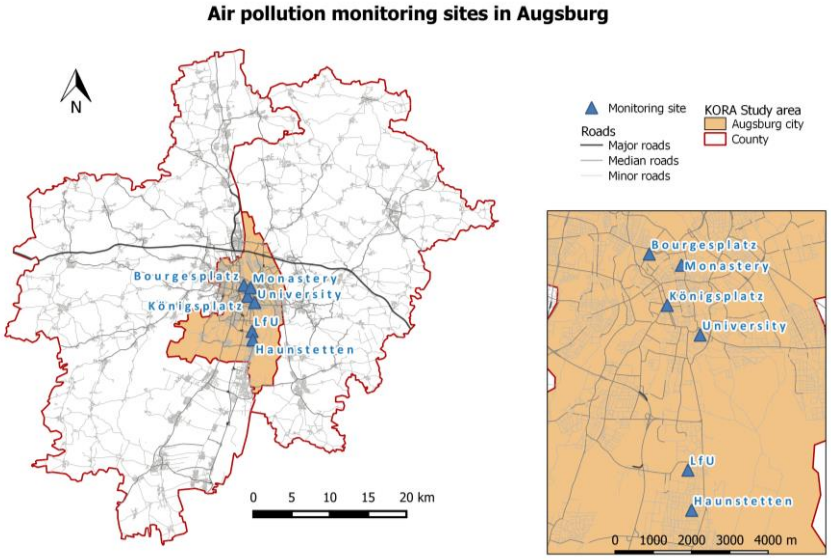

We generated the time series of daily pollutant concentrations covering the study period of KORA S4–FF4 as shown in the figure below. Using data from routine monitoring sites, we calculated the absolute differences in annual average concentrations between the period of each visit (01.01.2000–31.12.2000 for S4, 01.01.2007–31.12.2007 for F4, and 01.07.2013–30.06.2014 for FF4) and the period of ULTRA III measurements (01.03.2014–15.04.2015). To account for the difference in monitoring devices used at routine monitoring sites and in ULTRA III measurements, we calculated the ratio of average concentrations at the monitoring sites for the ULTRA III measurement period to average concentrations at the 20 measurement sites in ULTRA III, and calibrated the absolute difference by multiplying the absolute difference by the ratio. We then calculated for each study participant the back-extrapolated concentration at each visit by adding the calibrated absolute difference to the LUR-model-estimated ULTRA III annual average concentrations. The back-extrapolated air pollution concentrations reflected not only the spatial variation but also the temporal variation in exposure.

The mixed-effects models using back-extrapolated exposure were additionally adjusted for the year of visit to control for the potential temporal trend in both exposure and outcomes.

Time series of daily average concentrations of investigated air pollutants obtained from monitoring stations

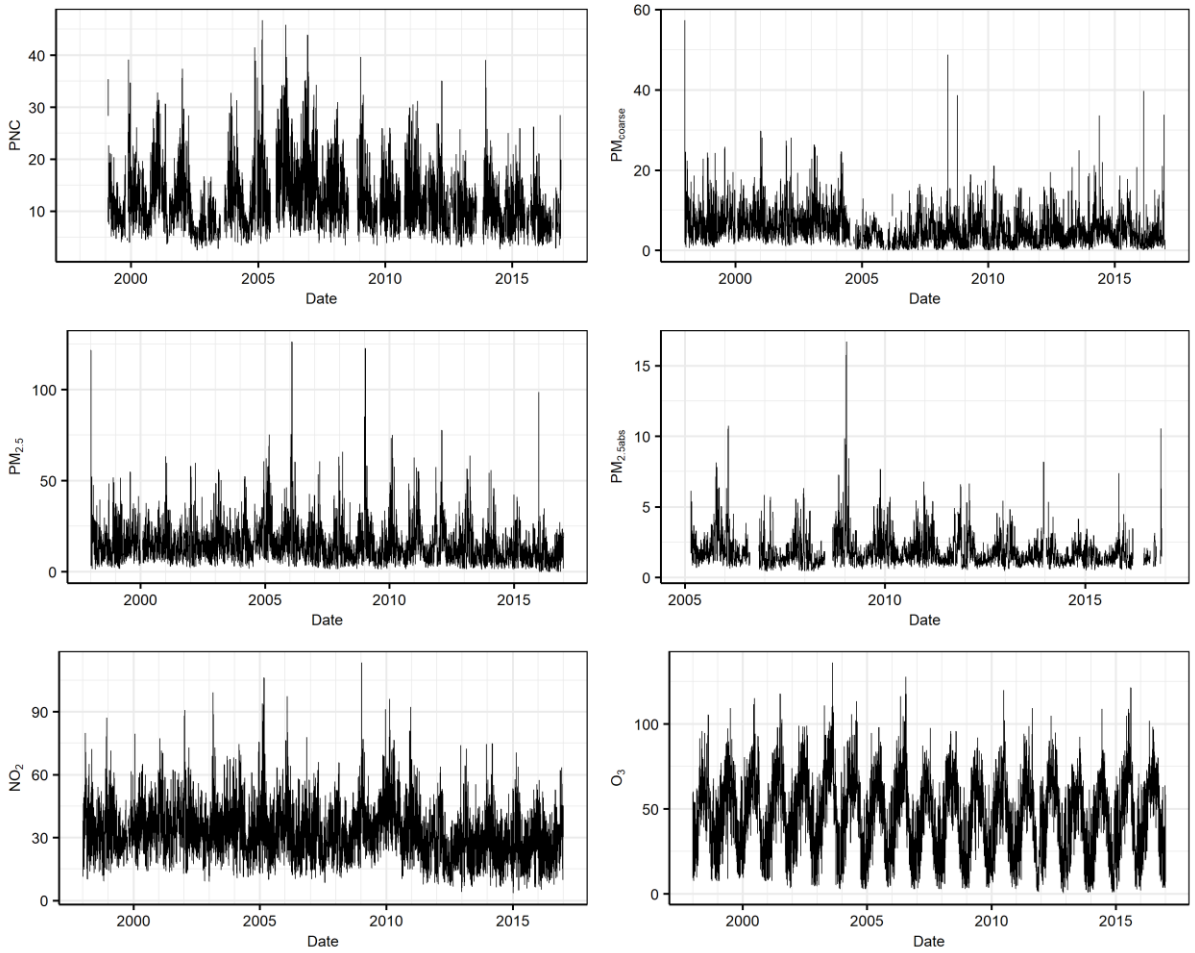

Table S1. Comparison of individual characteristics in KORA S4 among all KORA participants and participants included in the repeated measurements and annual rate of change analyses.

	KORA (*N* = 4,261)	Repeated measurements (*N* = 3,297)		Rate of change (*N* = 2,242)	
	Mean ± SD / *n* (%)	Mean ± SD / *n* (%)	*p*-value*	Mean ± SD / *n* (%)	*p*-value*
Age (years)	49·2 ± 13·9	50·3 ± 13·7	<0·001	49·5 ± 13·2	0·34
Sex (male)	2,090 (49)	1,590 (48)	0·49	1,086 (48)	0·66
Body mass index (kg/m^2)	27·2 ± 4·7	27·2 ± 4·5	0·94	26·8 ± 4·3	0·0091
Occupation (employed)	2,584 (61)	1,943 (59)	0·12	1,403 (63)	0·15
Education (high)	3,802 (89)	2,957 (90)	0·71	2,051 (91)	0·0085
Smoking pack-years	12·2 ± 19·6	11·6 ± 18·7	0·17	10·2 ± 16·9	<0·001
Smoking status			0·022		<0·001
Current smoker	1,118 (26)	776 (24)		467 (21)	
Former smoker	1,393 (33)	1,103 (33)		762 (34)	
Never smoker	1,745 (41)	1,418 (43)		1,013 (45)	
Alcohol consumption			0·22		<0·001
No	1,183 (28)	861 (26)		527 (24)	
Moderate	2,200 (52)	1,762 (54)		1,264 (56)	
High	860 (20)	669 (20)		448 (20)	
Physical activity			0·48		0·0013
Low	1,448 (34)	1,080 (33)		665 (30)	
Medium	1,933 (46)	1,532 (47)		1,081 (48)	
High	861 (20)	679 (20)		493 (22)	

*p-values indicate the significance of differences in characteristics among participants included in the repeated measurements and annual rate of change analyses compared with that among all KORA participants. p-values were derived from Kruskal-Wallis rank sum test for continuous variables and Chi-square test of independence for categorical variables.

Table S2. Distribution of the annual rate of change in biomarkers.

	Minimum	Q10	Q20	Q30	Q40	Median	Q60	Q70	Q80	Q90	Maximum	IQR
HOMA-IR (unit/year)	-6·20	-0·14	-0·07	-0·03	0·00	0·03	0·06	0·10	0·15	0·26	3·96	0.16
HOMA-B (unit/year)	-245·64	-8·62	-5·34	-3·30	-1·84	-0·47	0·72	1·90	3·68	6·66	94·52	6.78
Fasting insulin (μIU/ml/year)	-24·34	-0·59	-0·32	-0·16	-0·03	0·08	0·19	0·31	0·50	0·86	8·14	0.63
Fasting glucose (mg/dl/year)	-6·13	-0·78	-0·31	0·00	0·23	0·47	0·77	1·07	1·43	2·06	26·37	1.37

Table S3. Descriptive statistics of participant characteristics at the first and last visits stratified by the direction of annual rate of change in HOMA-IR.

	First visit			Last visit		
	Increasing HOMA-IR (*N* = 1,336)	**Unchanged / Decreasing HOMA-IR (*N* = 906)**	***p*-value***	**Increasing HOMA-IR (*N* = 1,336)**	**Unchanged / Decreasing HOMA-IR (*N* = 906)**	***p*-value***
HOMA-IR	2·2 ± 1·4	3·2 ± 4·1	<0·001	3·4 ± 2·5	2·0 ± 1·3	<0·001
HOMA-B	109·2 ± 56·5	148·8 ± 207·8	<0·001	125·5 ± 68·9	93·5 ± 54·2	<0·001
Fasting insulin (µIU/ml)	9·2 ± 5·2	13·2 ± 17·2	<0·001	13·1 ± 8·1	8·3 ± 4·8	<0·001
Fasting glucose (mg/dl)	94·3 ± 9·9	96·2 ± 10·4	<0·001	102·3 ± 18·0	96·2 ± 11·4	<0·001
Age (years)	54·2 ± 10·4	53·3 ± 10·8	0·052	62·5 ± 12·1	61·2 ± 12·2	0·015
Sex (male)	660 (49)	426 (47)	0·29	665 (49)	426 (47)	0·29
Body mass index (kg/m^2)	27·1 ± 4·2	27·3 ± 4·6	0·45	28·1 ± 4·8	27·3 ± 4·7	<0·001
Occupation (employed)	803 (60)	579 (64)	0·076	617 (46)	472 (52)	0·0068
Education (high)	1,223 (92)	828 (91)	0·96	1,223 (92)	828 (91)	0·96
Smoking pack-years	11·9 ± 19·2	10·0 ± 15·8	0·047	12·5 ± 20·0	10·5 ± 17·1	0·038
Smoking status			0·17			0·20
Current smoker	239 (18)	149 (16)		190 (14)	120 (13)	
Former smoker	516 (39)	327 (36)		566 (42)	358 (40)	
Never smoker	581 (43)	430 (48)		580 (44)	428 (47)	
Alcohol consumption			0·46			0·49
No	352 (27)	231 (25)		370 (28)	231 (25)	
Moderate	726 (54)	515 (57)		716 (54)	505 (56)	
High	258 (19)	160 (18)		250 (19)	170 (19)	
Physical activity			0·55			0·065
Low	386 (29)	280 (31)		418 (31)	242 (27)	
Medium	627 (47)	407 (45)		587 (44)	422 (46)	
High	323 (24)	219 (24)		331 (25)	242 (27)	
Diabetes status			0·0028			<0·001
Normal glucose tolerance	905 (69)	560 (62)		577 (44)	514 (59)	
Prediabetes	383 (29)	320 (36)		577 (44)	316 (36)	
Diabetes	33 (2)	16 (2)		149 (12)	45 (5)	

*p-values were derived from Kruskal-Wallis rank sum test for continuous variables and Chi-square test of independence for categorical variables.

Table S4. Absolute changes (95% CIs) in the annual rate of change of biomarkers at deciles of the distribution per IQR increase in air pollutant concentrations.

	Percentile	PNC	PM_{coarse}	$PM_{2.5}$	$PM_{2.5abs}$	NO_2	O_3
HOMA-IR	10th	0·007 (0·002, 0·012)	0·009 (0·002, 0·016)	0·007 (0·002, 0·012)	0·014 (0·008, 0·021)	0·012 (0·005, 0·019)	0·001 (-0·007, 0·008)
	20th	0·008 (0·004, 0·013)	0·008 (0·003, 0·014)	0·008 (0·003, 0·012)	0·014 (0·009, 0·020)	0·013 (0·006, 0·020)	0·001 (-0·005, 0·007)
	30th	0·005 (0·000, 0·009)	0·004 (-0·003, 0·011)	0·001 (-0·005, 0·007)	0·006 (-0·001, 0·013)	0·005 (-0·001, 0·012)	0·000 (-0·007, 0·007)
	40th	0·004 (0·000, 0·009)	0·004 (-0·003, 0·011)	0·001 (-0·006, 0·008)	0·010 (0·002, 0·018)	0·005 (-0·003, 0·013)	0·002 (-0·006, 0·009)
	50th	0·005 (-0·002, 0·011)	0·005 (-0·003, 0·013)	0·006 (-0·002, 0·013)	0·010 (0·001, 0·019)	0·006 (-0·003, 0·015)	0·000 (-0·008, 0·008)
	60th	0·009 (0·003, 0·014)	0·008 (0·000, 0·016)	0·009 (0·001, 0·017)	0·010 (0·000, 0·020)	0·009 (0·000, 0·018)	0·001 (-0·007, 0·009)
	70th	0·009 (0·003, 0·015)	0·011 (0·003, 0·018)	0·004 (-0·003, 0·012)	0·010 (0·000, 0·020)	0·008 (-0·002, 0·018)	0·007 (-0·001, 0·015)
	80th	0·005 (-0·004, 0·014)	0·011 (-0·001, 0·023)	0·000 (-0·012, 0·012)	0·005 (-0·009, 0·018)	0·000 (-0·013, 0·013)	0·014 (0·002, 0·025)
	90th	0·000 (-0·010, 0·010)	0·011 (-0·003, 0·026)	-0·015 (-0·030, -0·001)	0·005 (-0·009, 0·018)	-0·004 (-0·020, 0·012)	0·015 (-0·004, 0·033)
HOMA-B	10th	0·175 (-0·072, 0·421)	0·199 (-0·116, 0·514)	0·232 (-0·025, 0·488)	-0·041 (-0·438, 0·356)	0·166 (-0·193, 0·525)	0·053 (-0·236, 0·343)
	20th	0·207 (0·000, 0·414)	0·216 (-0·059, 0·491)	0·296 (0·020, 0·572)	0·337 (0·093, 0·582)	0·240 (-0·078, 0·558)	-0·017 (-0·308, 0·274)
	30th	0·210 (0·048, 0·372)	0·292 (0·041, 0·544)	0·389 (0·152, 0·626)	0·298 (0·020, 0·576)	0·337 (0·057, 0·618)	0·161 (-0·106, 0·428)
	40th	0·140 (-0·113, 0·393)	0·194 (-0·113, 0·501)	0·224 (-0·083, 0·531)	0·268 (-0·107, 0·643)	0·285 (-0·070, 0·640)	-0·018 (-0·332, 0·295)
	50th	0·231 (-0·020, 0·482)	0·424 (0·107, 0·740)	0·435 (0·100, 0·770)	0·574 (0·185, 0·963)	0·528 (0·161, 0·894)	0·121 (-0·237, 0·479)
	60th	0·287 (0·009, 0·564)	0·451 (0·100, 0·801)	0·237 (-0·088, 0·561)	0·481 (0·087, 0·875)	0·435 (0·053, 0·817)	0·080 (-0·278, 0·437)
	70th	0·265 (0·023, 0·507)	0·462 (0·095, 0·830)	0·335 (0·015, 0·656)	0·460 (0·091, 0·829)	0·399 (-0·015, 0·813)	0·113 (-0·237, 0·462)
	80th	0·464 (0·176, 0·751)	0·745 (0·450, 1·041)	0·303 (-0·102, 0·707)	0·691 (0·269, 1·112)	0·532 (0·148, 0·917)	0·330 (0·010, 0·650)
	90th	0·544 (-0·070, 1·157)	0·919 (0·286, 1·552)	0·173 (-0·418, 0·764)	0·500 (-0·095, 1·095)	0·020 (-0·732, 0·773)	0·506 (-0·126, 1·137)
Fasting insulin	10th	0·035 (0·012, 0·057)	0·032 (0·006, 0·059)	0·013 (-0·014, 0·039)	0·042 (0·009, 0·074)	0·041 (0·008, 0·073)	-0·004 (-0·031, 0·023)
	20th	0·037 (0·019, 0·055)	0·036 (0·011, 0·060)	0·036 (0·012, 0·060)	0·057 (0·027, 0·088)	0·049 (0·020, 0·077)	0·000 (-0·024, 0·023)
	30th	0·030 (0·014, 0·046)	0·031 (0·014, 0·048)	0·023 (0·002, 0·043)	0·038 (0·012, 0·063)	0·042 (0·016, 0·067)	-0·003 (-0·027, 0·021)
	40th	0·030 (0·008, 0·053)	0·030 (0·000, 0·060)	0·031 (0·001, 0·060)	0·048 (0·012, 0·084)	0·041 (0·007, 0·075)	0·017 (-0·013, 0·046)
	50th	0·025 (0·004, 0·045)	0·034 (0·002, 0·065)	0·031 (0·001, 0·061)	0·055 (0·019, 0·091)	0·040 (0·003, 0·077)	0·004 (-0·027, 0·035)
	60th	0·042 (0·018, 0·065)	0·051 (0·019, 0·083)	0·032 (0·004, 0·060)	0·055 (0·019, 0·090)	0·055 (0·023, 0·087)	0·018 (-0·012, 0·049)
	70th	0·021 (-0·004, 0·046)	0·038 (0·007, 0·069)	0·013 (-0·019, 0·045)	0·030 (-0·006, 0·066)	0·029 (-0·007, 0·064)	0·028 (0·000, 0·056)
	80th	0·025 (-0·008, 0·058)	0·038 (0·001, 0·075)	0·011 (-0·034, 0·056)	0·040 (-0·012, 0·091)	0·021 (-0·028, 0·071)	0·029 (-0·012, 0·071)
	90th	0·021 (-0·011, 0·052)	0·067 (0·009, 0·125)	-0·038 (-0·083, 0·006)	0·014 (-0·045, 0·074)	0·014 (-0·038, 0·065)	0·056 (0·003, 0·110)
Fasting glucose	10th	-0·028 (-0·092, 0·035)	-0·020 (-0·088, 0·047)	-0·047 (-0·116, 0·023)	-0·001 (-0·096, 0·095)	-0·001 (-0·090, 0·087)	0·045 (-0·033, 0·124)
	20th	0·022 (-0·033, 0·078)	0·004 (-0·071, 0·079)	0·005 (-0·068, 0·078)	0·083 (-0·008, 0·174)	0·049 (-0·042, 0·141)	-0·009 (-0·084, 0·067)
	30th	0·011 (-0·040, 0·063)	0·001 (-0·063, 0·066)	0·004 (-0·060, 0·067)	0·051 (-0·026, 0·129)	0·031 (-0·041, 0·103)	-0·042 (-0·107, 0·022)
	40th	-0·001 (-0·055, 0·052)	-0·039 (-0·095, 0·017)	-0·001 (-0·064, 0·061)	0·010 (-0·069, 0·088)	-0·021 (-0·094, 0·052)	-0·011 (-0·066, 0·045)
	50th	0·029 (-0·025, 0·082)	-0·020 (-0·085, 0·045)	-0·011 (-0·078, 0·057)	0·042 (-0·037, 0·120)	0·016 (-0·056, 0·089)	0·002 (-0·062, 0·066)
	60th	0·025 (-0·022, 0·072)	0·034 (-0·020, 0·087)	-0·053 (-0·114, 0·009)	0·060 (-0·007, 0·127)	0·049 (-0·016, 0·114)	-0·003 (-0·064, 0·059)
	70th	0·019 (-0·038, 0·076)	0·012 (-0·056, 0·081)	-0·058 (-0·130, 0·015)	0·033 (-0·052, 0·117)	0·012 (-0·068, 0·092)	0·007 (-0·059, 0·072)
	80th	0·020 (-0·053, 0·093)	-0·006 (-0·095, 0·083)	-0·029 (-0·120, 0·062)	-0·003 (-0·121, 0·115)	-0·019 (-0·135, 0·097)	-0·007 (-0·112, 0·098)
	90th	-0·056 (-0·136, 0·024)	-0·048 (-0·137, 0·041)	-0·055 (-0·168, 0·058)	-0·056 (-0·168, 0·056)	-0·083 (-0·185, 0·019)	-0·093 (-0·190, 0·004)

Quantile regression models for the annual rate of change were adjusted for baseline levels of the investigated biomarker, age (baseline), sex, BMI (baseline), annual rate of change in BMI, educational attainment (baseline), occupational status (baseline), smoking status (baseline), smoking pack-years (baseline), annual rate of change in smoking pack-years, physical activity (baseline), and an indicator for the visits used in the calculation of the rate of change. An IQR increase was $2{\cdot}0\times10^3$/cm^3 for PNC, 1·4 μg/m^3 for PM_{coarse}, 1·4 μg/m^3 for $PM_{2.5}$, $0{\cdot}3\times10^{-5}$/m for $PM_{2.5abs}$, 7·1 μg/m^3 for NO_2, and 3·5 μg/m^3 for O_3.

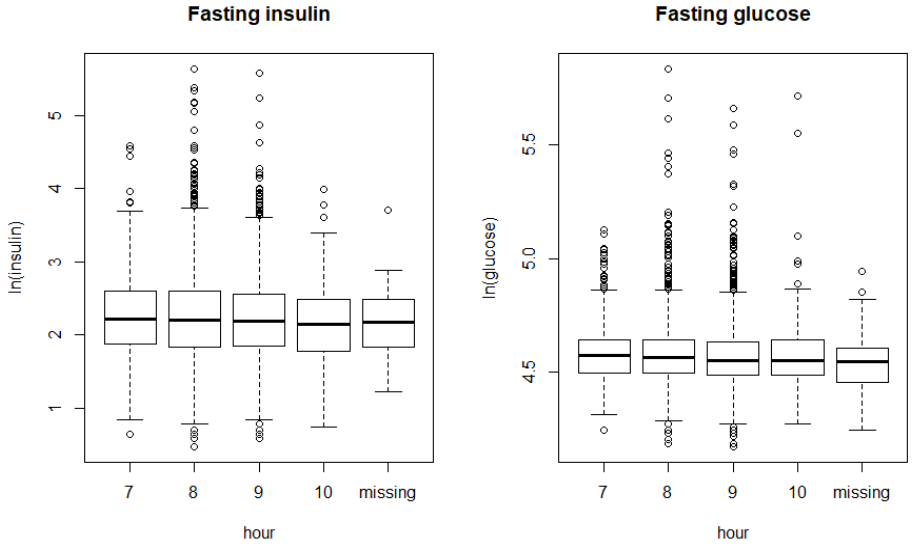

Figure S1. Distribution of ln-transformed fasting insulin and fasting glucose stratified by the hour of blood withdrawal.

Blood samples drawn during 7:00 AM–8:00 AM (hour=7): *N*=645; 8:00 AM–9:00 AM (hour=8): *N*=2,969; 9:00 AM–10:00 AM (hour=9): *N*=2,122; 10:00 AM–11:00 AM (hour=10): *N*=238; without documented time (missing): *N*=34.

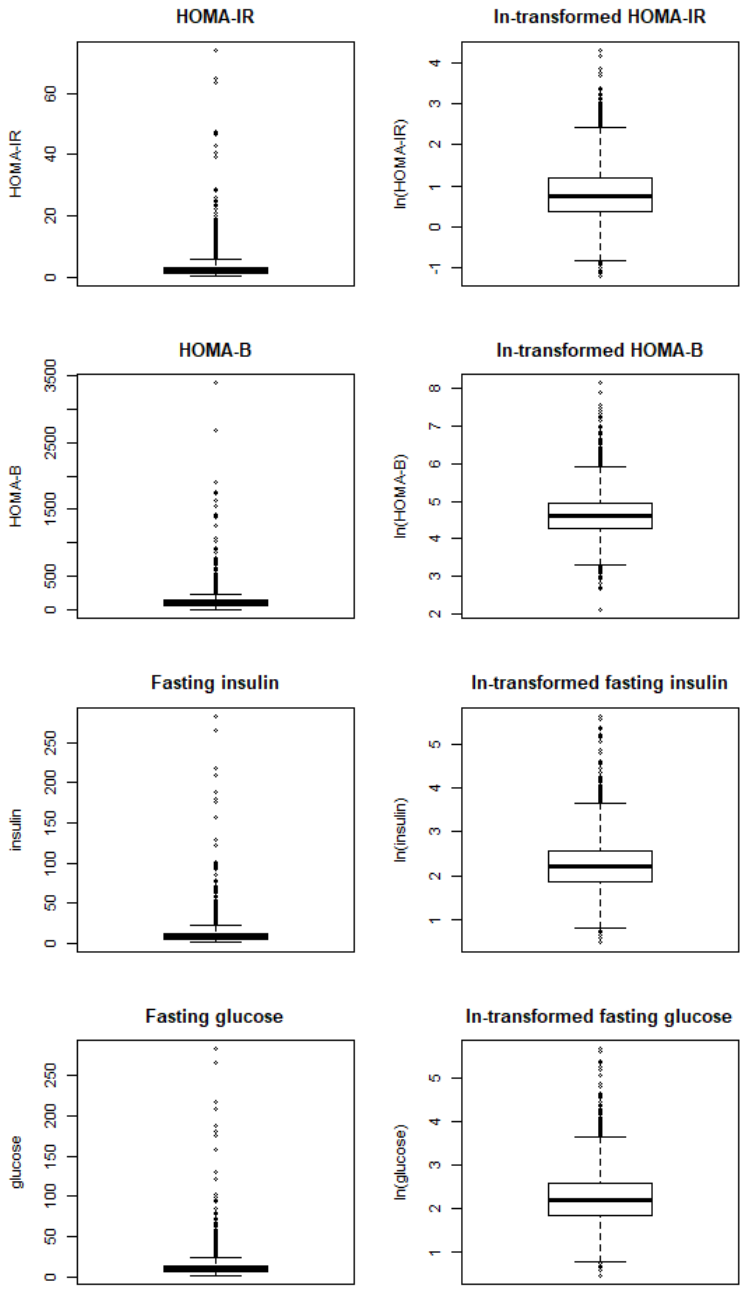

Figure S2. Boxplots of biomarker concentrations on the original and natural log (ln)-transformed scales.

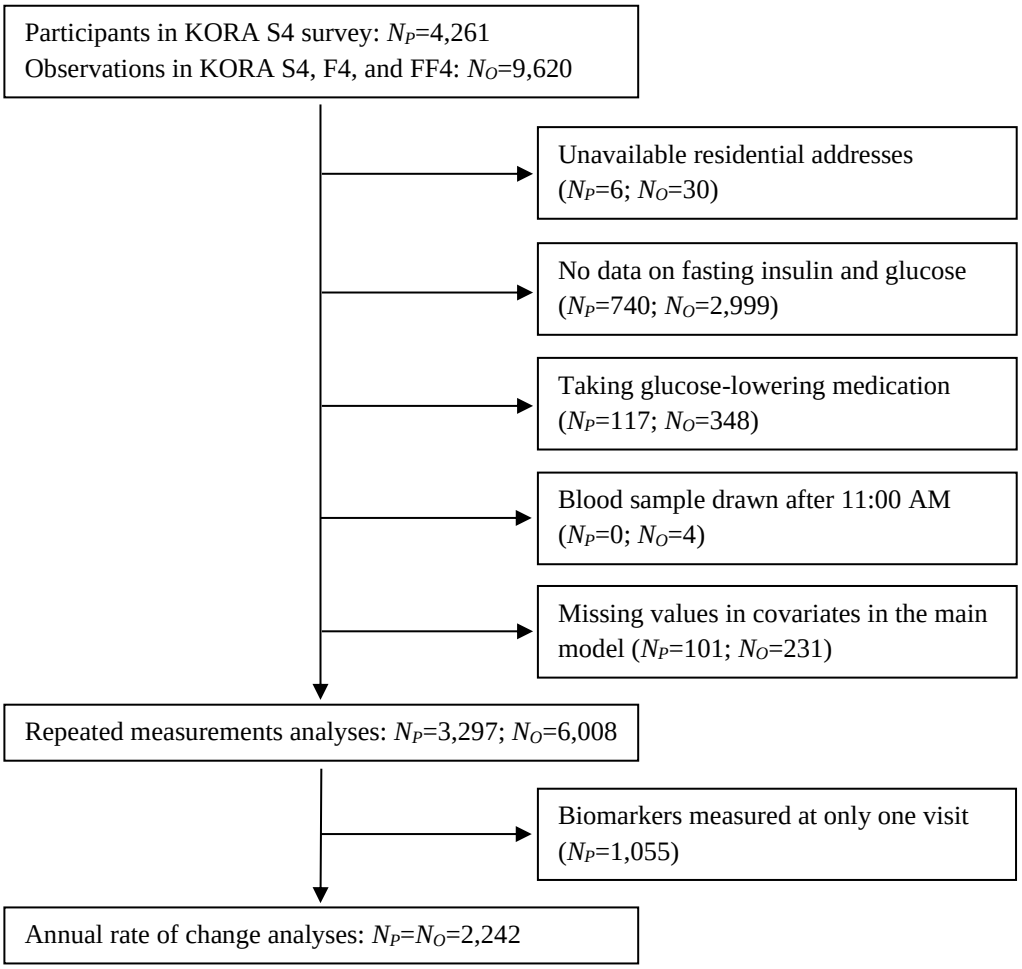

Figure S3. Flow chart of the exclusion process.

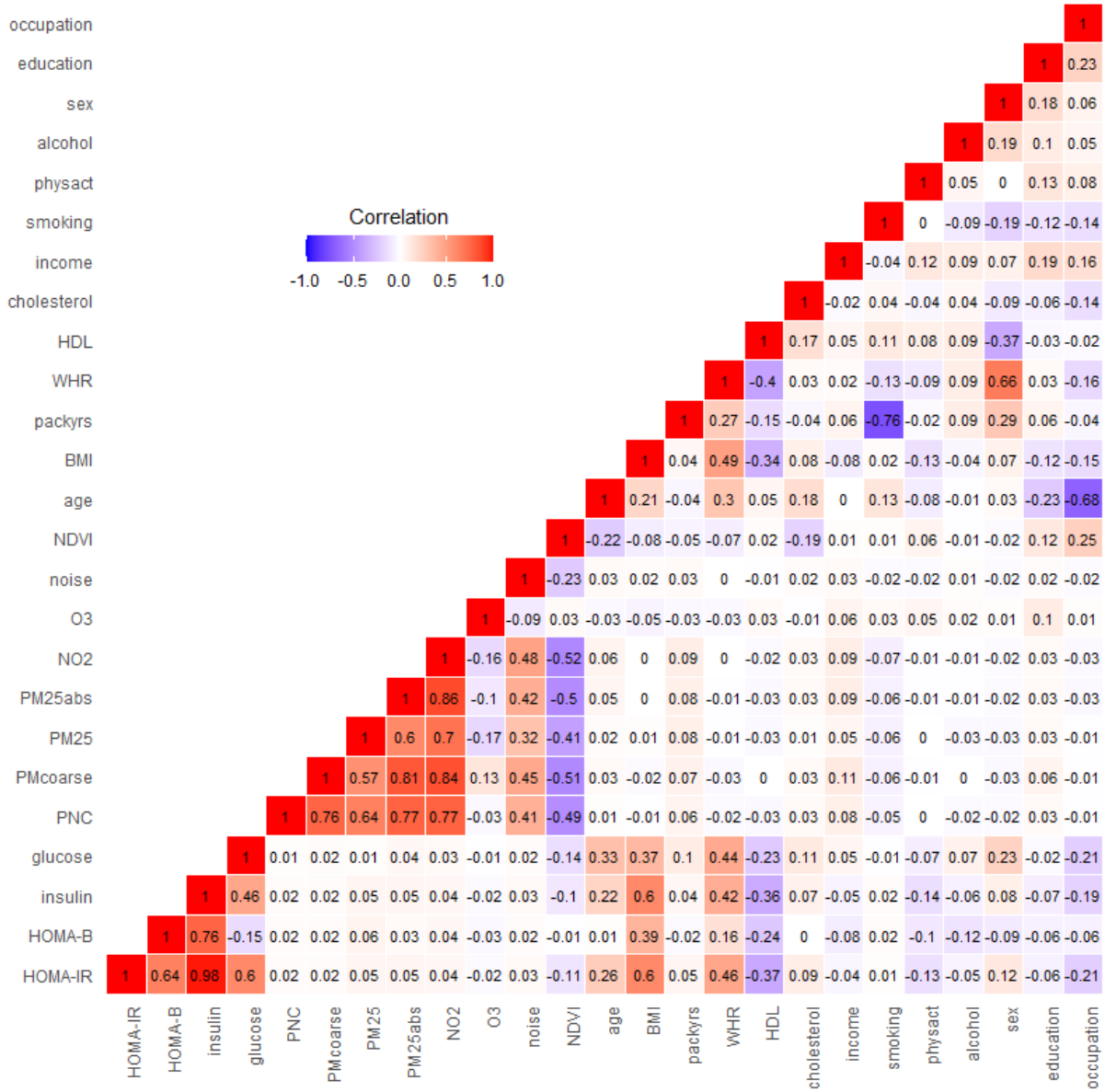

Figure S4. Correlation between outcome, exposure, and covariate variables.
Correlation coefficients in the figure were (1) Spearman's rank correlation coefficients for two continuous variables; (2) Kendall rank correlation coefficients for one continuous and one ordinal variable, or two ordinal variables; (3) Point-Biserial correlation coefficients for one dichotomous and one continuous/ordinal variable; (4) Cramer's V correlation coefficients for two categorical variables. BMI=body mass index; HDL= high-density lipoproteins; income=per capita income; HOMA-IR=homeostasis model assessment of insulin resistance; HOMA-B=homeostasis model assessment of β-cell function; NDVI=normalized difference vegetation index; NO_2=nitrogen dioxide, O_3=ozone; PM_{coarse}= particulate matter with an aerodynamic diameter between 2·5 μm and 10 μm; $PM_{2·5}$=particulate matter with an aerodynamic diameter ≤ 2·5 μm; $PM_{2·5abs}$=$PM_{2·5}$ absorbance; PNC=particle number concentration; WHR=waist-hip-ratio

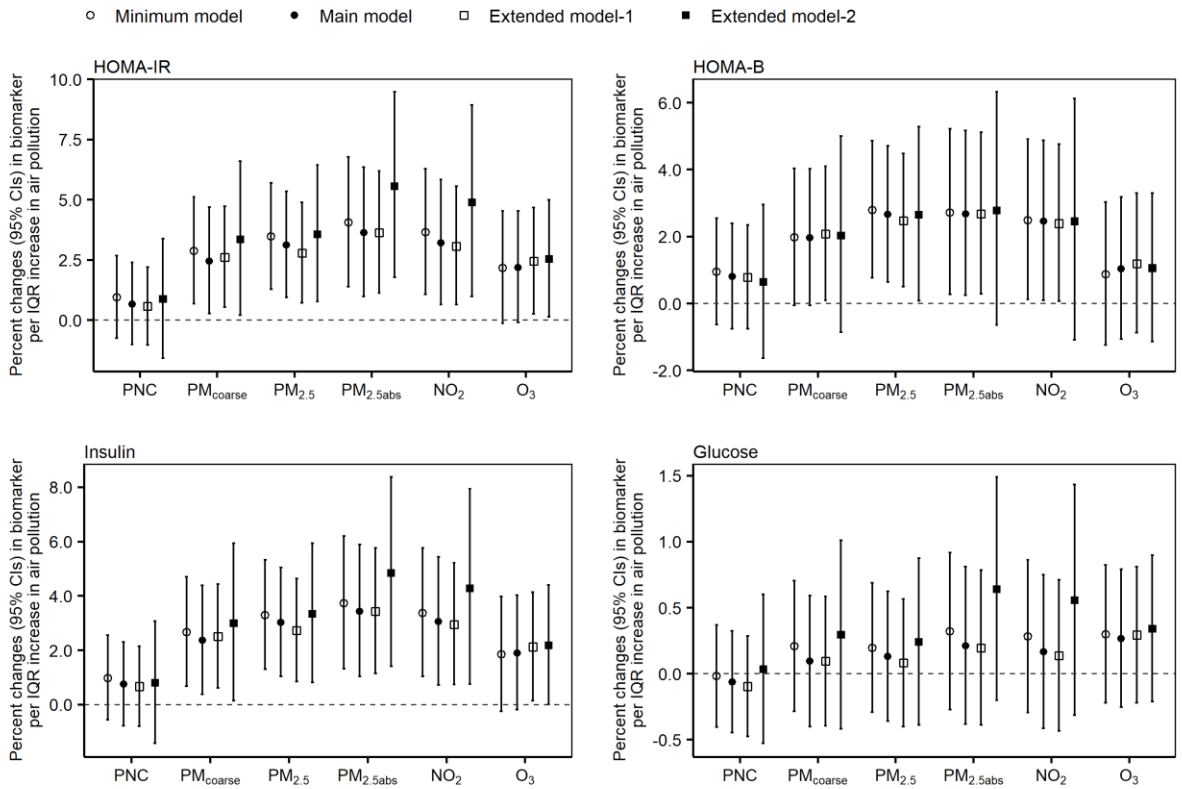

Figure S5. Percent changes (95% CIs) in the repeated measurements of biomarkers per IQR increase in air pollutant concentrations in models with different adjustments of covariates.

Minimum models were adjusted for age, sex, BMI, season, visits; main models were further adjusted for educational attainment, occupational status, smoking status, smoking pack-years, alcohol consumption, and physical activity; extended model-1 was further adjusted for waist-hip-ratio, high-density lipoprotein, and total cholesterol in addition to covariates in main models; extended model-2 were further adjusted for NDVI and noise in addition to covariates in main models. An IQR increase was $2{\cdot}0\times10^{3}$/cm^3 for PNC, 1·4 μg/m^3 for PM_{coarse}, 1·4 μg/m^3 for $PM_{2{\cdot}5}$, $0{\cdot}3\times10^{-5}$/m for $PM_{2{\cdot}5abs}$, 7·1 μg/m^3 for NO_2, and 3·5 μg/m^3 for O_3.

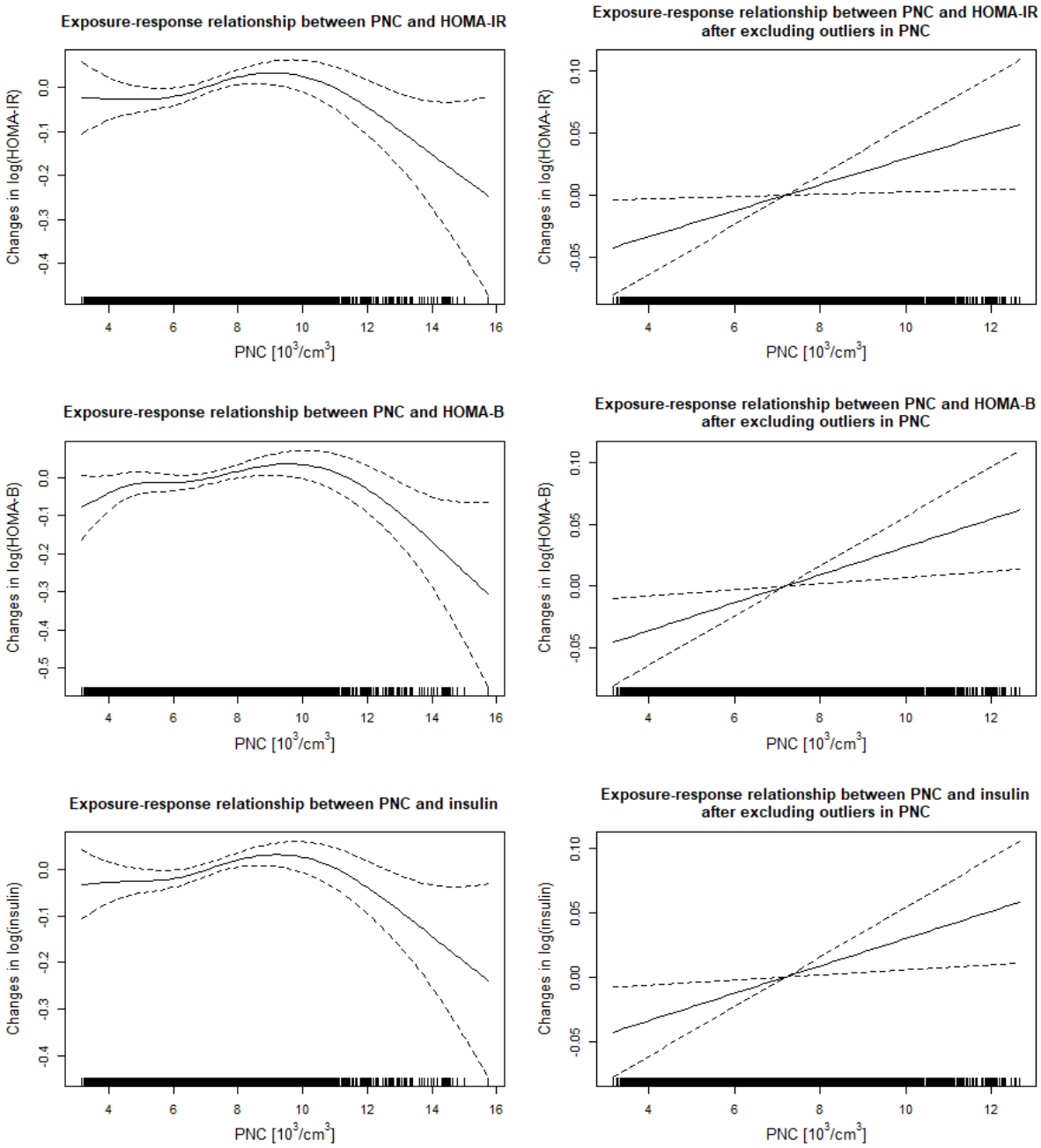

Figure S6. Exposure-response relationships between PNC and HOMA-IR, HOMA-B, and fasting insulin. Panels on the left side show the exposure-response relationship for the whole range of PNC; panels on the right side show the exposure-response relationship for PNC < $12{\cdot}7\times10^3/cm^3$.

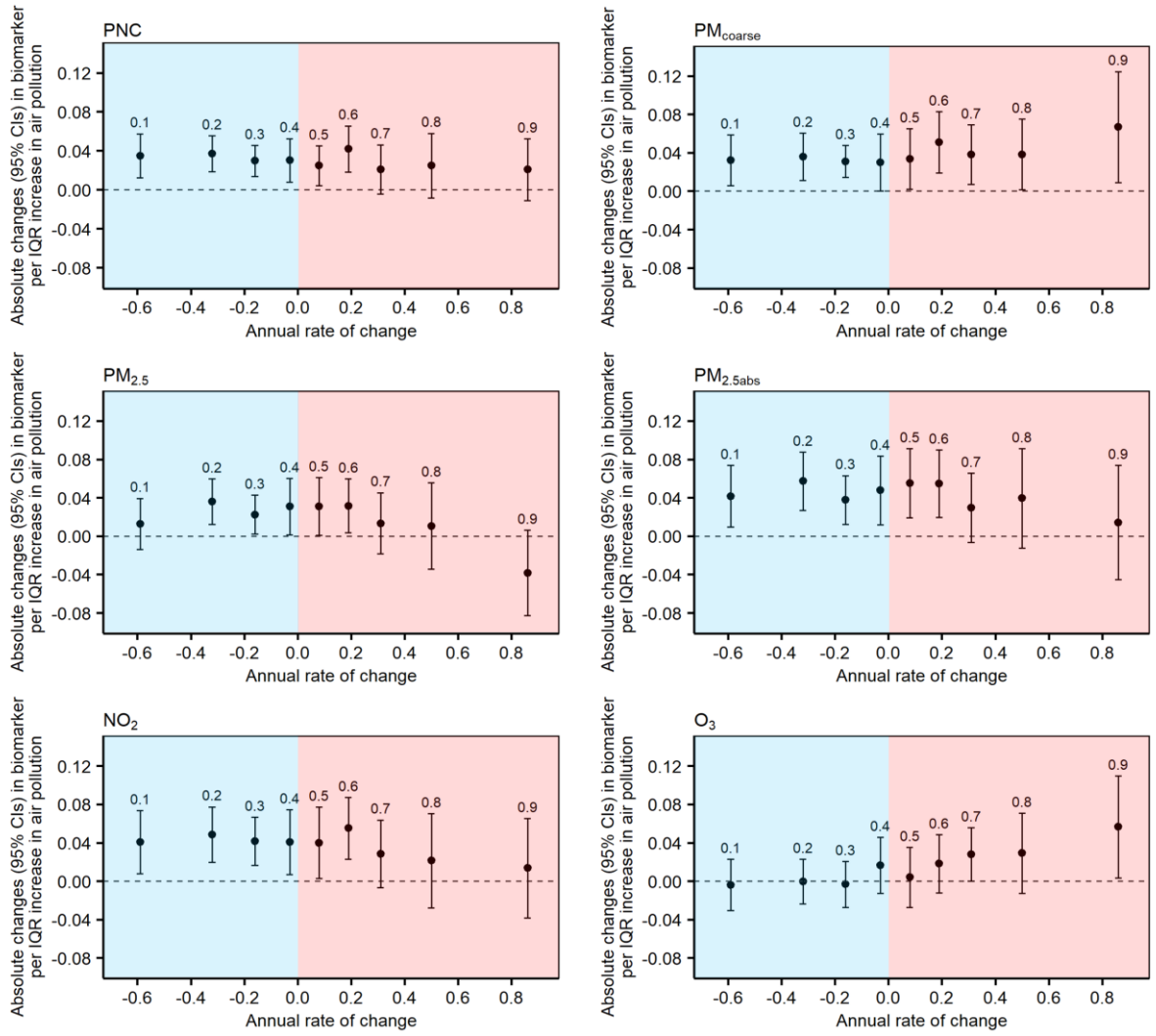

Figure S7. Absolute changes (95% CIs) in the annual rate of change in fasting insulin at deciles of the distribution per IQR increase in air pollutant concentrations.

Quantile regression models for the annual rate of change were adjusted for baseline levels of the investigated biomarker, age (baseline), sex, BMI (baseline), annual rate of change in BMI, educational attainment (baseline), occupational status (baseline), smoking status (baseline), smoking pack-years (baseline), annual rate of change in smoking pack-years, physical activity (baseline), and an indicator for the visits used in the calculation of the rate of change. Blue shaded area on the left side indicates decreasing insulin secretion over years (annual rate of change below zero); red shaded area on the right side indicates increasing insulin secretion over years (annual rate of change above zero). Values (i.e. 0·1–0·9) above the error bars indicate the deciles of the distribution of annual rate of change. An IQR increase was $2{\cdot}0\times10^{3}$/cm^3 for PNC, 1·4 μg/m^3 for PM$_{coarse}$, 1·4 μg/m^3 for PM$_{2·5}$, $0{\cdot}3\times10^{-5}$/m for PM$_{2·5abs}$, 7·1 μg/m^3 for NO$_2$, and 3·5 μg/m^3 for O$_3$.

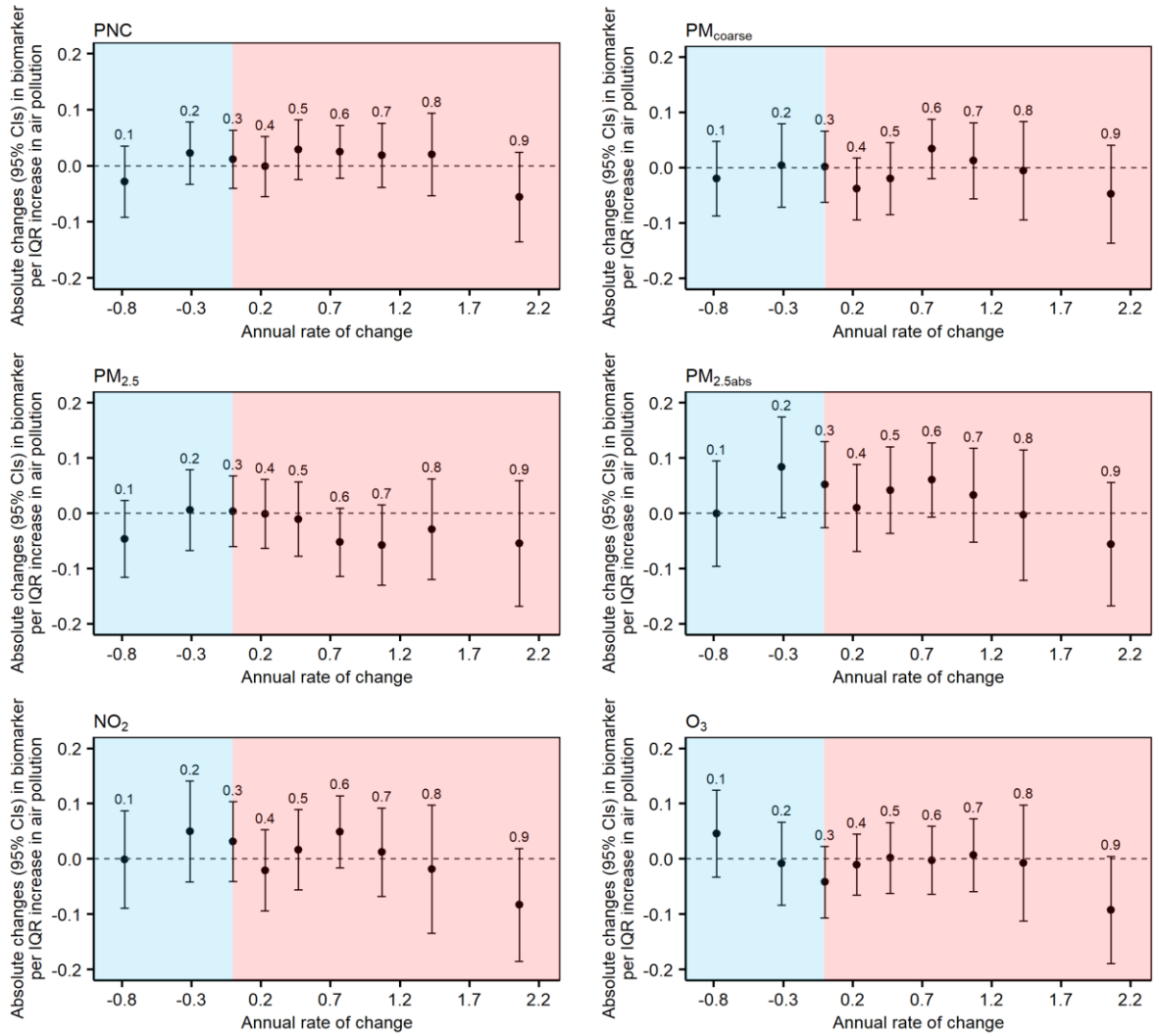

Figure S8. Absolute changes (95% CIs) in the annual rate of change in fasting glucose at deciles of the distribution per IQR increase in air pollutant concentrations.

Quantile regression models for the annual rate of change were adjusted for baseline levels of the investigated biomarker, age (baseline), sex, BMI (baseline), annual rate of change in BMI, educational attainment (baseline), occupational status (baseline), smoking status (baseline), smoking pack-years (baseline), annual rate of change in smoking pack-years, physical activity (baseline), and an indicator for the visits used in the calculation of the rate of change. Blue shaded area on the left side indicates decreasing fasting glucose concentrations over years (annual rate of change below zero); red shaded area on the right side indicates increasing fasting glucose concentrations over years (annual rate of change above zero). Values (i.e. 0·1–0·9) above the error bars indicate the deciles of the distribution of annual rate of change. An IQR increase was $2{\cdot}0\times10^{3}$/cm^3 for PNC, 1·4 μg/m^3 for PM$_{coarse}$, 1·4 μg/m^3 for PM$_{2·5}$, $0{\cdot}3\times10^{-5}$/m for PM$_{2·5abs}$, 7·1 μg/m^3 for NO$_2$, and 3·5 μg/m^3 for O$_3$.

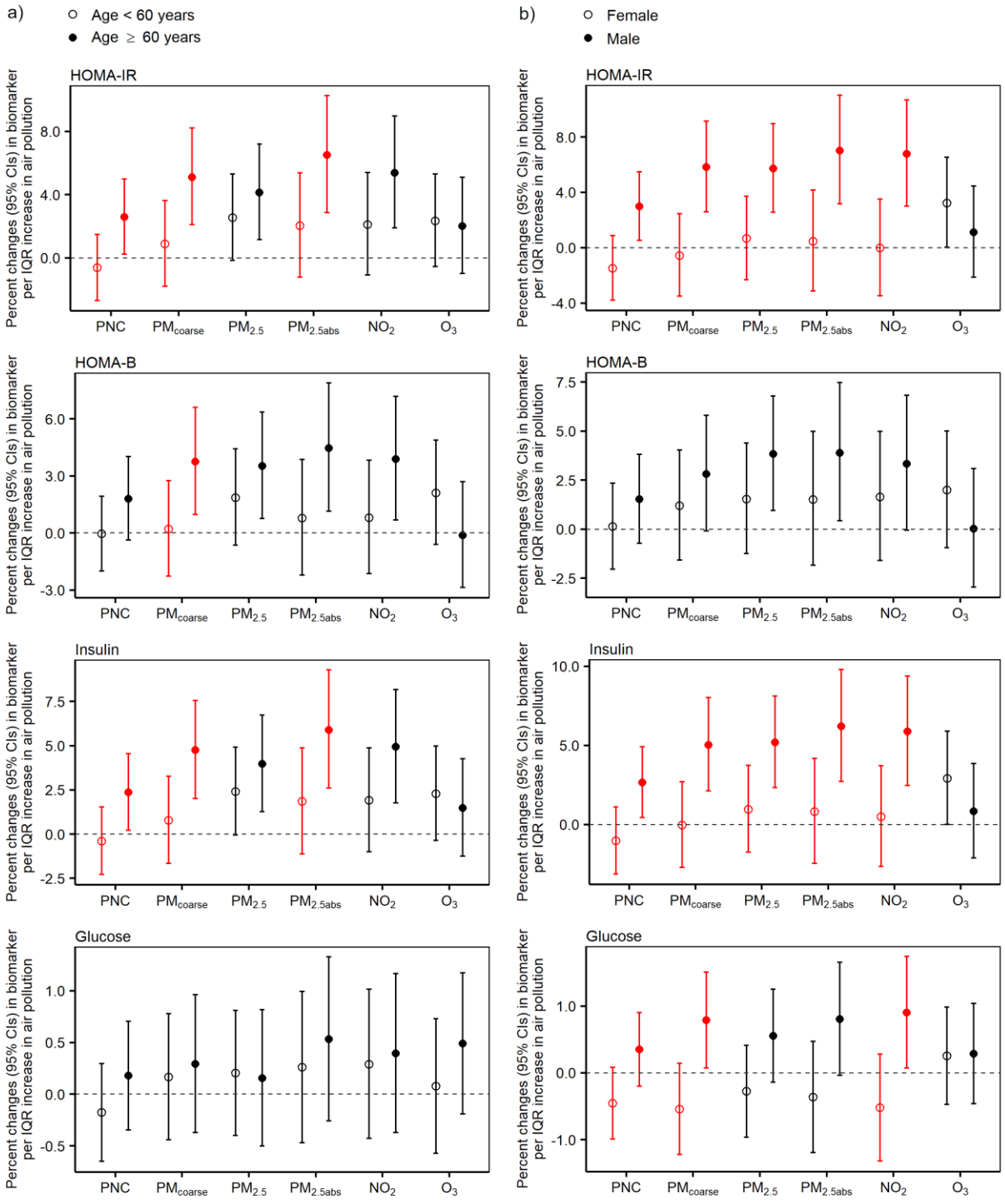

Figure S9. Percent changes (95% CIs) in repeated measurements of biomarkers per IQR increase in air pollutant concentrations by a) age and b) sex.

Panels on the left side show the effect modification by age (age < 60 years: number of observations (*N*) = 3,019, age ≥ 60 years: *N*=2,989); panels on the right side show the effect modification by sex (female: *N*=3,083, male: *N*=2,925). Error bars in red indicate significant differences in effect estimates between subgroups (*p*-value for the interaction term < 0·05). An IQR increase was $2{\cdot}0\times10^3$/cm^3 for PNC, 1·4 µg/m^3 for PM_{coarse}, 1·4 µg/m^3 for $PM_{2{\cdot}5}$, $0{\cdot}3\times10^{-5}$/m for $PM_{2{\cdot}5abs}$, 7·1 µg/m^3 for NO_2, and 3·5 µg/m^3 for O_3.

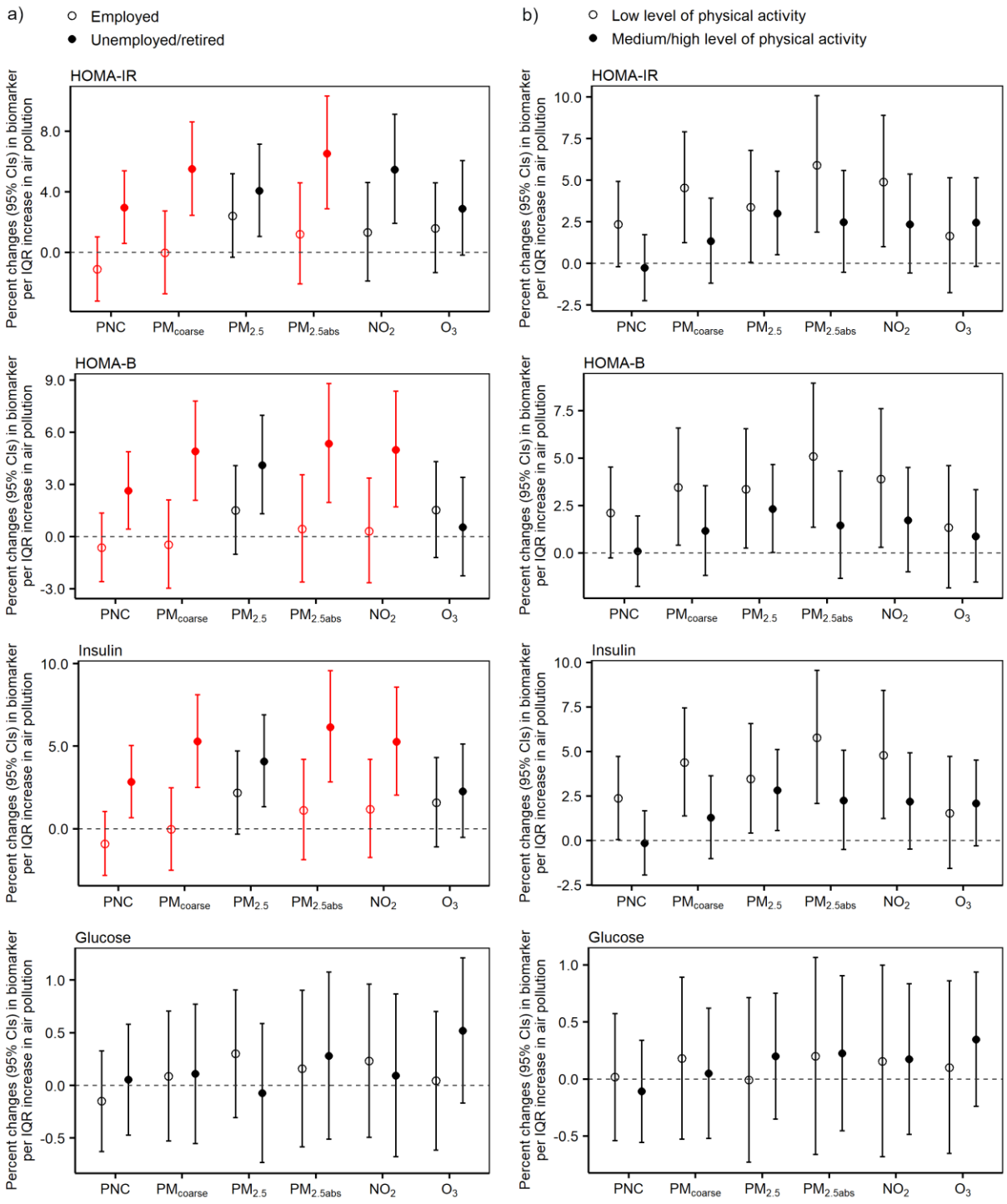

Figure S10. Percent changes (95% CIs) in repeated measurements of biomarkers per IQR increase in air pollutant concentrations by a) occupational status and b) physical activity.

Panels on the left side show effect modification by occupational status (employed: *N*=3,053, unemployed/retired: *N*=2,955); panels on the right side show the effect modification by physical activity (low level: *N*=1,893, medium/high level: *N*=4,115). Error bars in red indicate significant differences in effect estimates between subgroups (*p*-value for the interaction term < 0·05). An IQR increase was $2{\cdot}0\times10^3$/cm^3 for PNC, 1·4 μg/m^3 for PM_{coarse}, 1·4 μg/m^3 for $PM_{2{\cdot}5}$, $0{\cdot}3\times10^{-5}$/m for $PM_{2{\cdot}5abs}$, 7·1 μg/m^3 for NO_2, and 3·5 μg/m^3 for O_3.

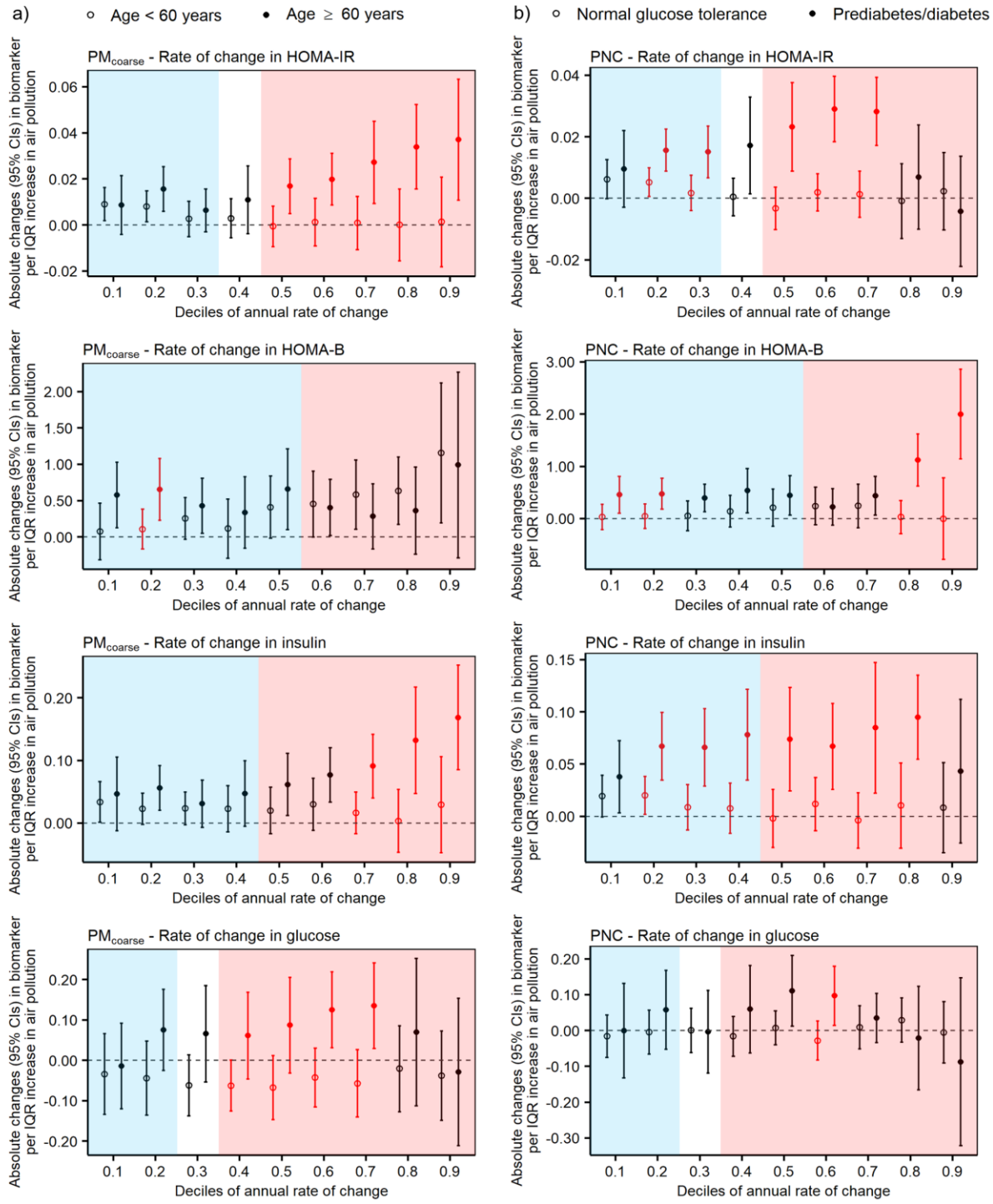

Figure S11. Absolute changes (95% CIs) in the annual rate of change in biomarkers per IQR increase in air pollutant concentrations by a) age and b) diabetes status.

Panels on the left side show the effect modification by age at baseline (age < 60 years: *N*=1,519, age ≥ 60 years: *N*=723); panels on the right side show the effect modification by diabetes status at baseline (normal glucose tolerance: *N*=1,465, prediabetes/diabetes: *N*=752). Blue shaded area on the left side indicates annual rate of change below zero; red shaded area on the right side indicates annual rate of change above zero; unshaded area in the middle indicates stable biomarker levels over years. Error bars in red indicate significant differences in effect estimates between subgroups (*p*-value for the interaction term < 0·05). An IQR increase was $2{\cdot}0\times10^{3}$/cm^3 for PNC, 1·4 μg/m^3 for PM_{coarse}, 1·4 μg/m^3 for $PM_{2{\cdot}5}$, $0{\cdot}3\times10^{-5}$/m for $PM_{2{\cdot}5abs}$, 7·1 μg/m^3 for NO_2, and 3·5 μg/m^3 for O_3.

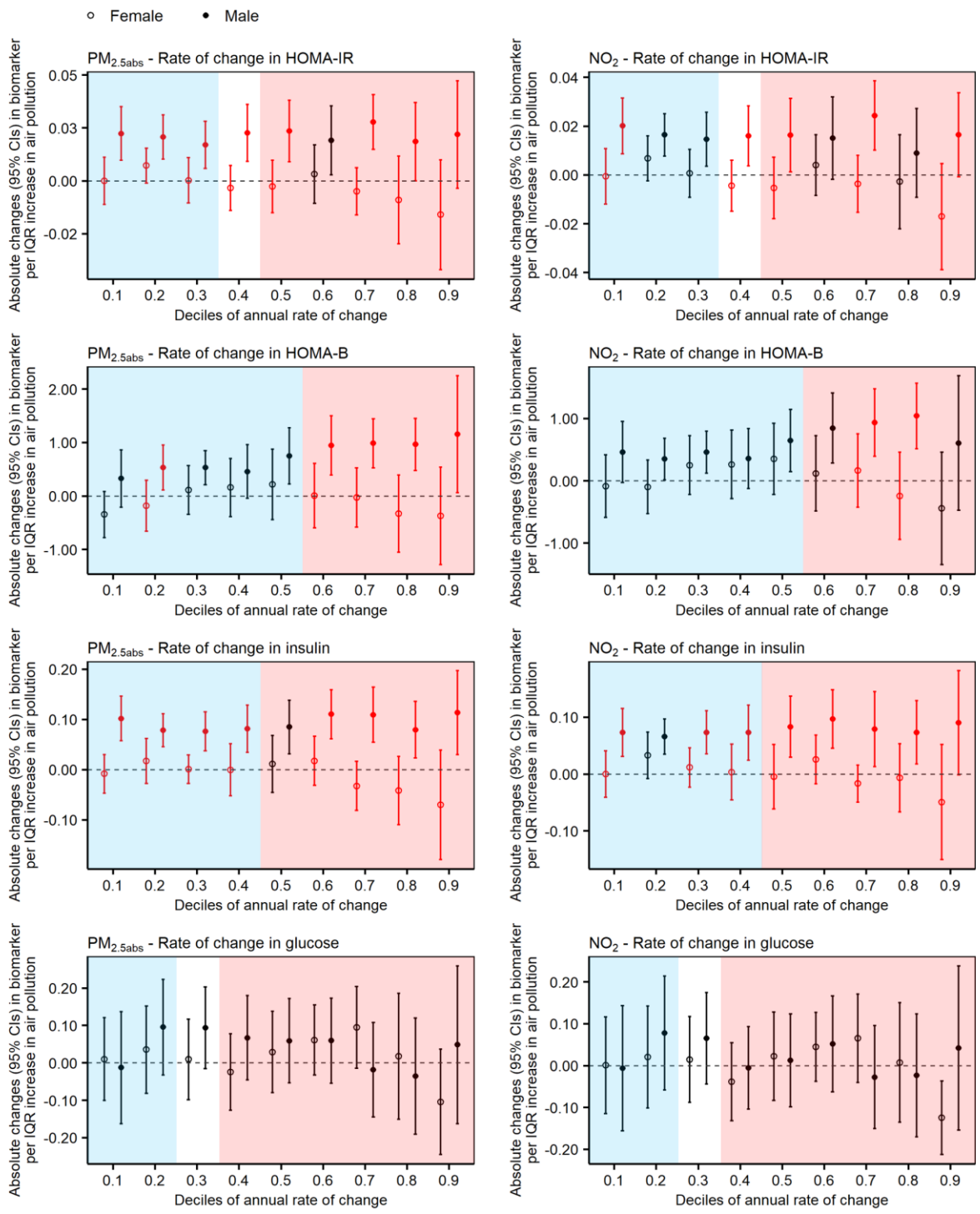

Figure S12. Absolute changes (95% CIs) in the annual rate of change in HOMA-IR and fasting insulin per IQR increase in air pollutant concentrations by sex.

Blue shaded area on the left side indicates annual rate of change below zero; red shaded area on the right side indicates annual rate of change above zero; unshaded area in the middle indicates stable biomarker levels over years. Error bars in red indicate significant differences in effect estimates between subgroups (*p*-value for the interaction term < 0·05). Numbers of females and males were 1,156 and 1,086, respectively. An IQR increase was $2{\cdot}0\times10^{3}$/cm^3 for PNC, 1·4 μg/m^3 for PM_{coarse}, 1·4 μg/m^3 for $PM_{2{\cdot}5}$, $0{\cdot}3\times10^{-5}$/m for $PM_{2{\cdot}5abs}$, 7·1 μg/m^3 for NO_2, and 3·5 μg/m^3 for O_3.

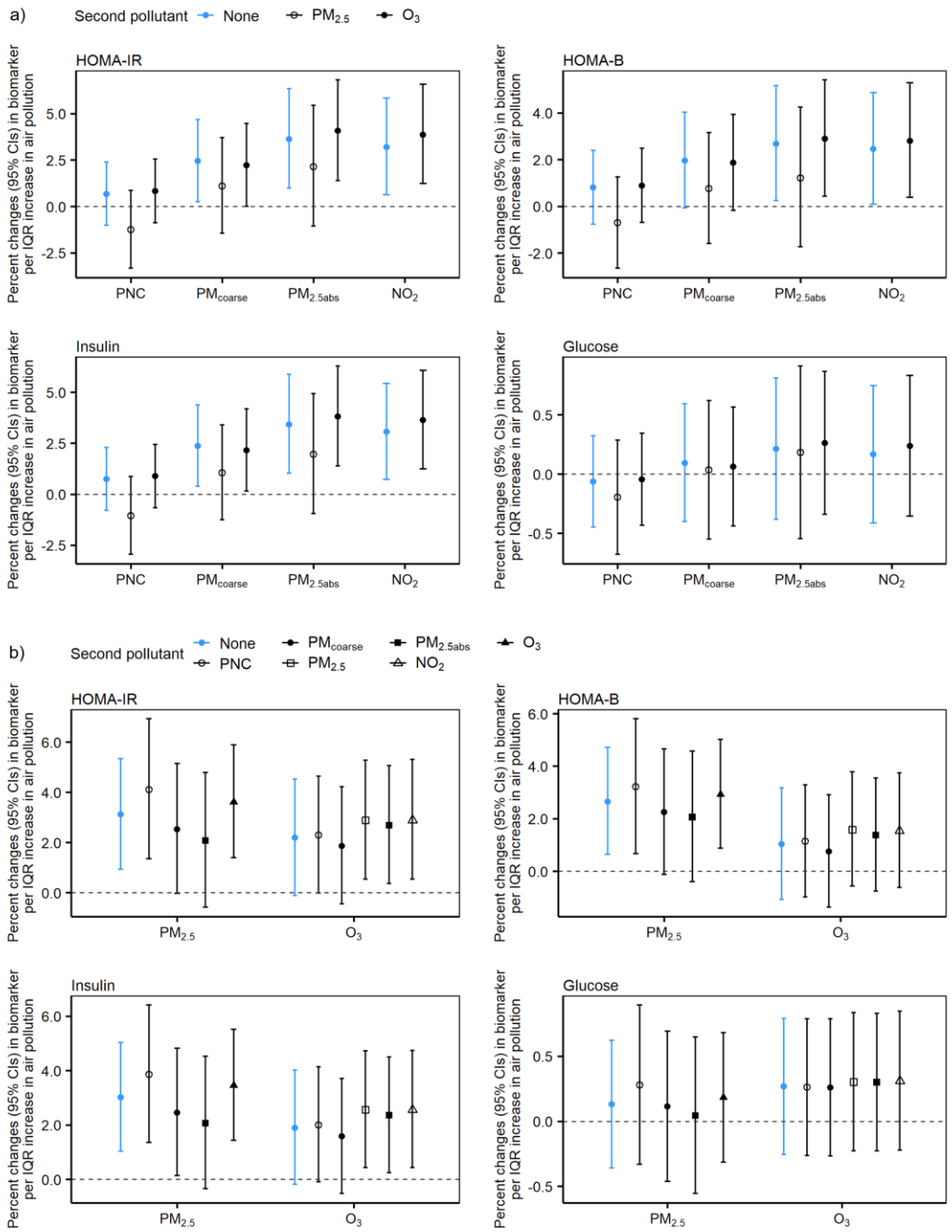

Figure S13. Percent changes (95% CIs) in repeated measurements of biomarkers per IQR increase in air pollutant concentrations in two-pollutant models.

Error bars in blue represent the effect estimates in single-pollutant models. An IQR increase was $2{\cdot}0\times10^{3}$/cm^{3} for PNC, 1·4 μg/m^{3} for PM_{coarse}, 1·4 μg/m^{3} for $PM_{2{\cdot}5}$, $0{\cdot}3\times10^{-5}$/m for $PM_{2{\cdot}5abs}$, 7·1 μg/m^{3} for NO_2, and 3·5 μg/m^{3} for O_3.

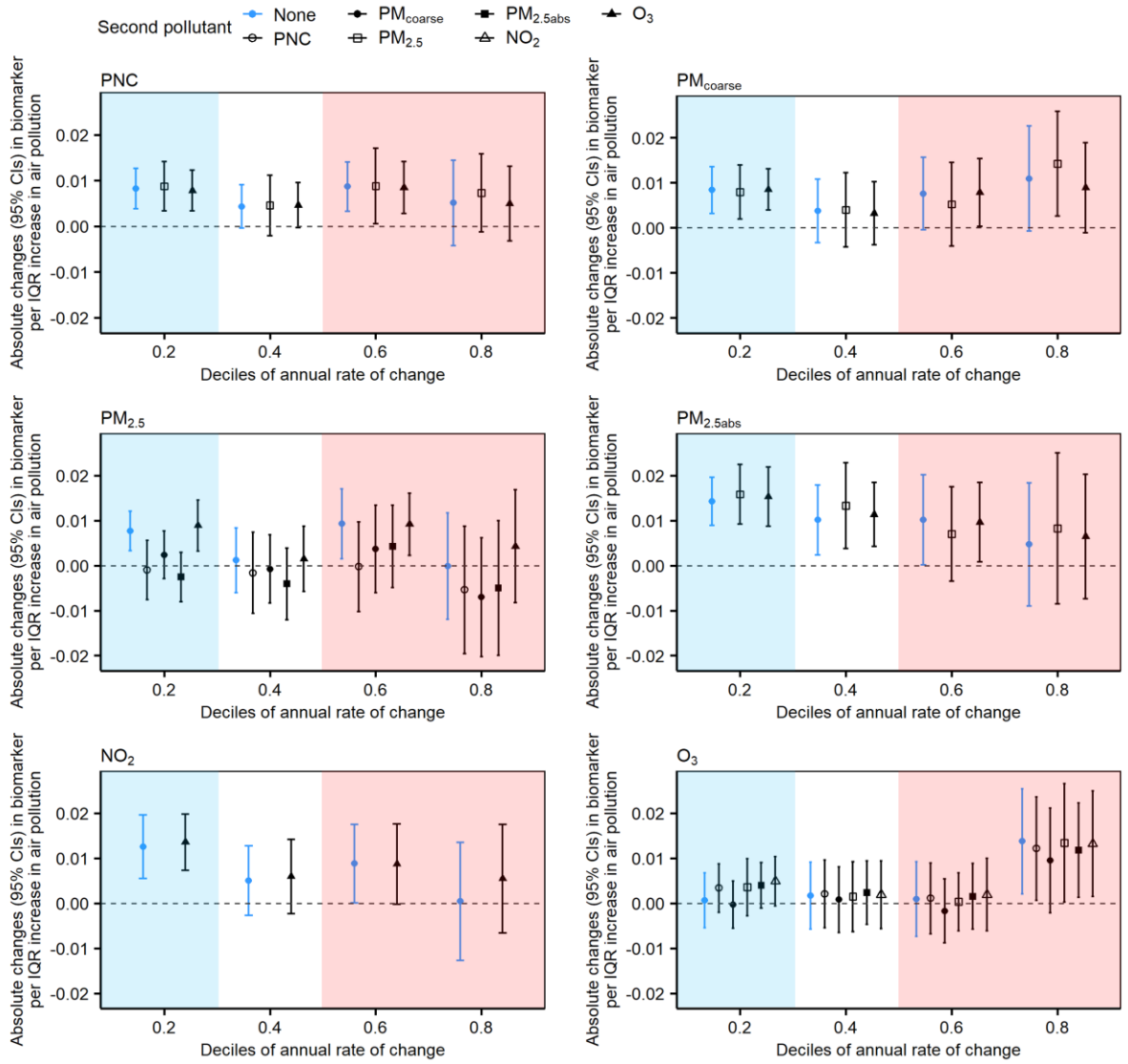

Figure S14. Absolute changes (95% CIs) in the annual rate of change in HOMA-IR at different percentiles of the distribution per IQR increase in air pollutant concentrations in two-pollutant models.
Blue shaded area on the left side indicates annual rate of change below zero; red shaded area on the right side indicates annual rate of change above zero; unshaded area in the middle indicates stable biomarker levels over years. Error bars in blue represent the effect estimates in single-pollutant models. An IQR increase was $2{\cdot}0\times10^{3}$/cm^3 for PNC, 1·4 μg/m^3 for PM$_{coarse}$, 1·4 μg/m^3 for PM$_{2\cdot5}$, $0{\cdot}3\times10^{-5}$/m for PM$_{2\cdot5abs}$, 7·1 μg/m^3 for NO$_2$, and 3·5 μg/m^3 for O$_3$.

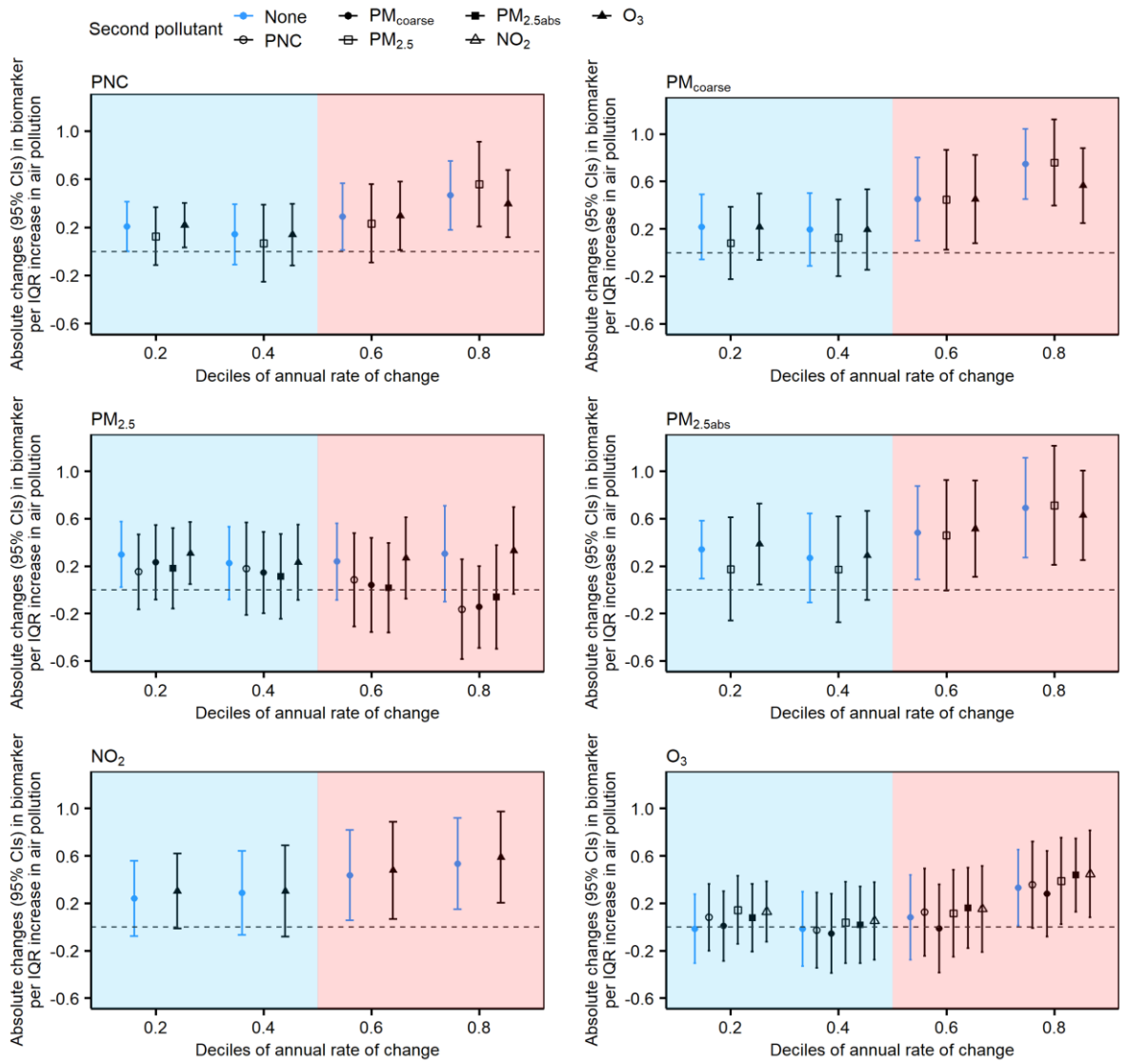

Figure S15. Absolute changes (95% CIs) in the annual rate of change in HOMA-B at different percentiles of the distribution per IQR increase in air pollutant concentrations in two-pollutant models.
Blue shaded area on the left side indicates annual rate of change below zero; red shaded area on the right side indicates annual rate of change above zero. Error bars in blue represent the effect estimates in single-pollutant models. An IQR increase was $2{\cdot}0\times10^{3}$/cm^3 for PNC, 1·4 μg/m^3 for PM$_{coarse}$, 1·4 μg/m^3 for PM$_{2·5}$, $0{\cdot}3\times10^{-5}$/m for PM$_{2·5abs}$, 7·1 μg/m^3 for NO$_2$, and 3·5 μg/m^3 for O$_3$.

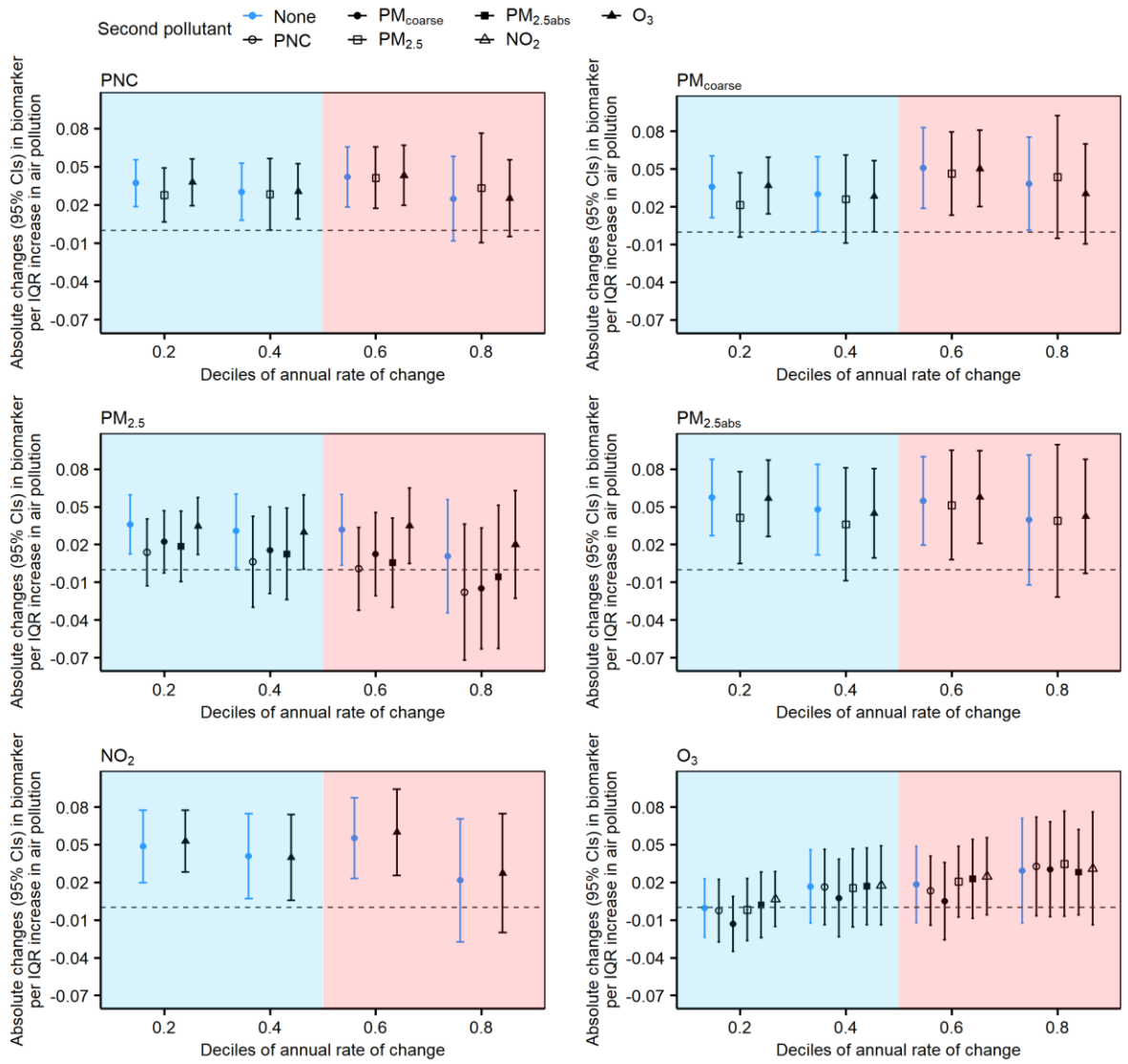

Figure S16. Absolute changes (95% CIs) in the annual rate of change in fasting insulin at different percentiles of the distribution per IQR increase in air pollutant concentrations in two-pollutant models.
Blue shaded area on the left side indicates annual rate of change below zero; red shaded area on the right side indicates annual rate of change above zero. Error bars in blue represent the effect estimates in single-pollutant models. An IQR increase was $2{\cdot}0\times10^{3}$/cm^3 for PNC, 1·4 μg/m^3 for PM_{coarse}, 1·4 μg/m^3 for $PM_{2\cdot5}$, $0{\cdot}3\times10^{-5}$/m for $PM_{2\cdot5abs}$, 7·1 μg/m^3 for NO_2, and 3·5 μg/m^3 for O_3.

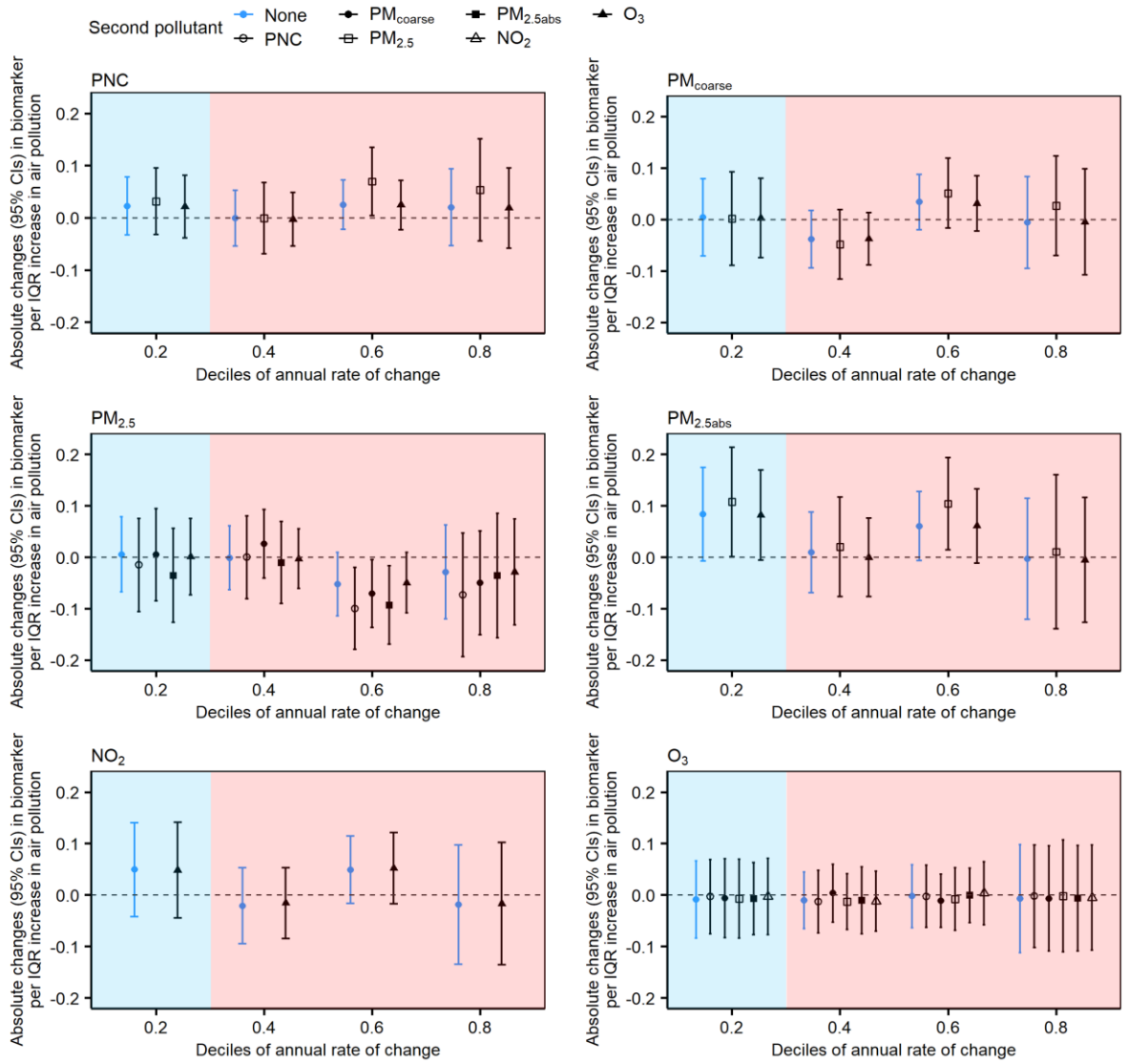

Figure S17. Absolute changes (95% CIs) in the annual rate of change in fasting glucose at different percentiles of the distribution per IQR increase in air pollutant concentrations in two-pollutant models.
Blue shaded area on the left side indicates annual rate of change below zero; red shaded area on the right side indicates annual rate of change above zero. Error bars in blue represent the effect estimates in single-pollutant models. An IQR increase was $2{\cdot}0\times10^{3}$/cm^3 for PNC, 1·4 μg/m^3 for PM$_{coarse}$, 1·4 μg/m^3 for PM$_{2{\cdot}5}$, $0{\cdot}3\times10^{-5}$/m for PM$_{2{\cdot}5abs}$, 7·1 μg/m^3 for NO$_2$, and 3·5 μg/m^3 for O$_3$.

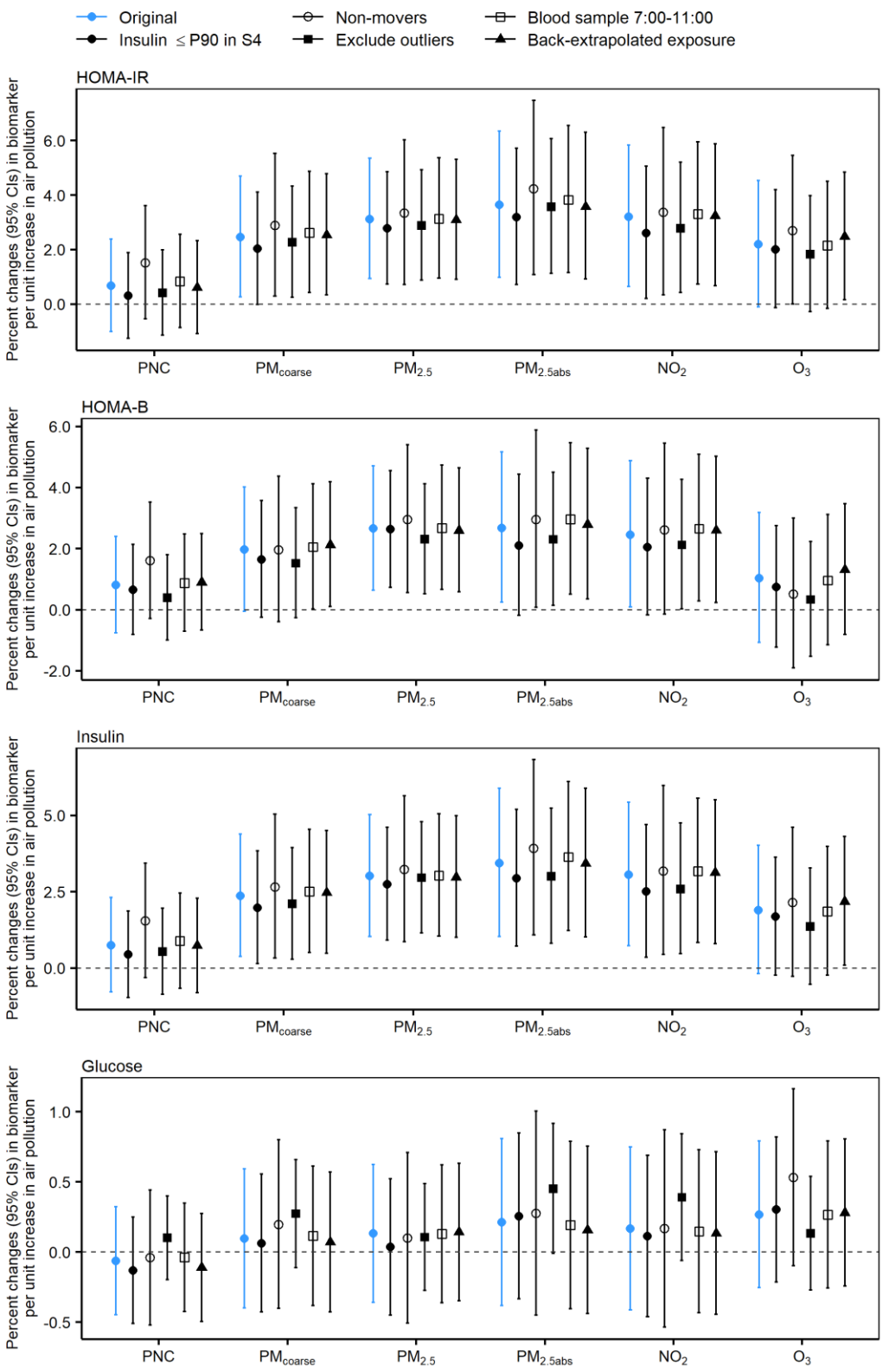

Figure S18. Percent changes (95% CIs) in repeated measurements of biomarkers per IQR increase in air pollutant concentrations in sensitivity analyses.

Original: main ME model (number of observations remained in the analysis (*N*) = 6,008). Insulin ≤ P90 in S4: observations with fasting insulin concentrations ≤ the 90th percentile (21·9 μIU/mL) in KORA S4 (*N*=5,783). Non-movers: participants who did not move during S4 to FF4 (*N*=4,748). Exclude outliers: exclude outliers in outcome variables (*N*=5,911 for HOMA-IR, *N*=5,886 for HOMA-B, *N*=5,907 for insulin, *N*=5,829 for glucose). Blood sample 7:00-11:00: blood samples drawn between 7:00 AM and 11:00 AM (*N*=5,974). Back-extrapolated exposure: use back-extrapolated exposure data with further adjustment for the year of examinations (*N*=6,008).

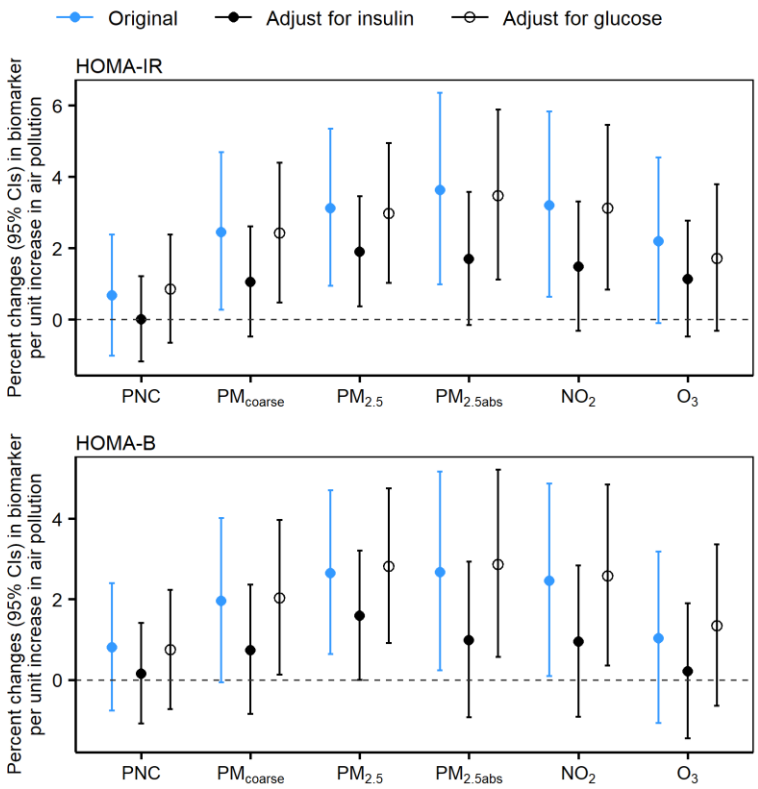

Figure S19. Percent changes (95% CIs) in repeated measurements of HOMA-IR and HOMA-B per IQR increase in air pollutant concentrations in models with further adjustment for fasting insulin or fasting glucose.

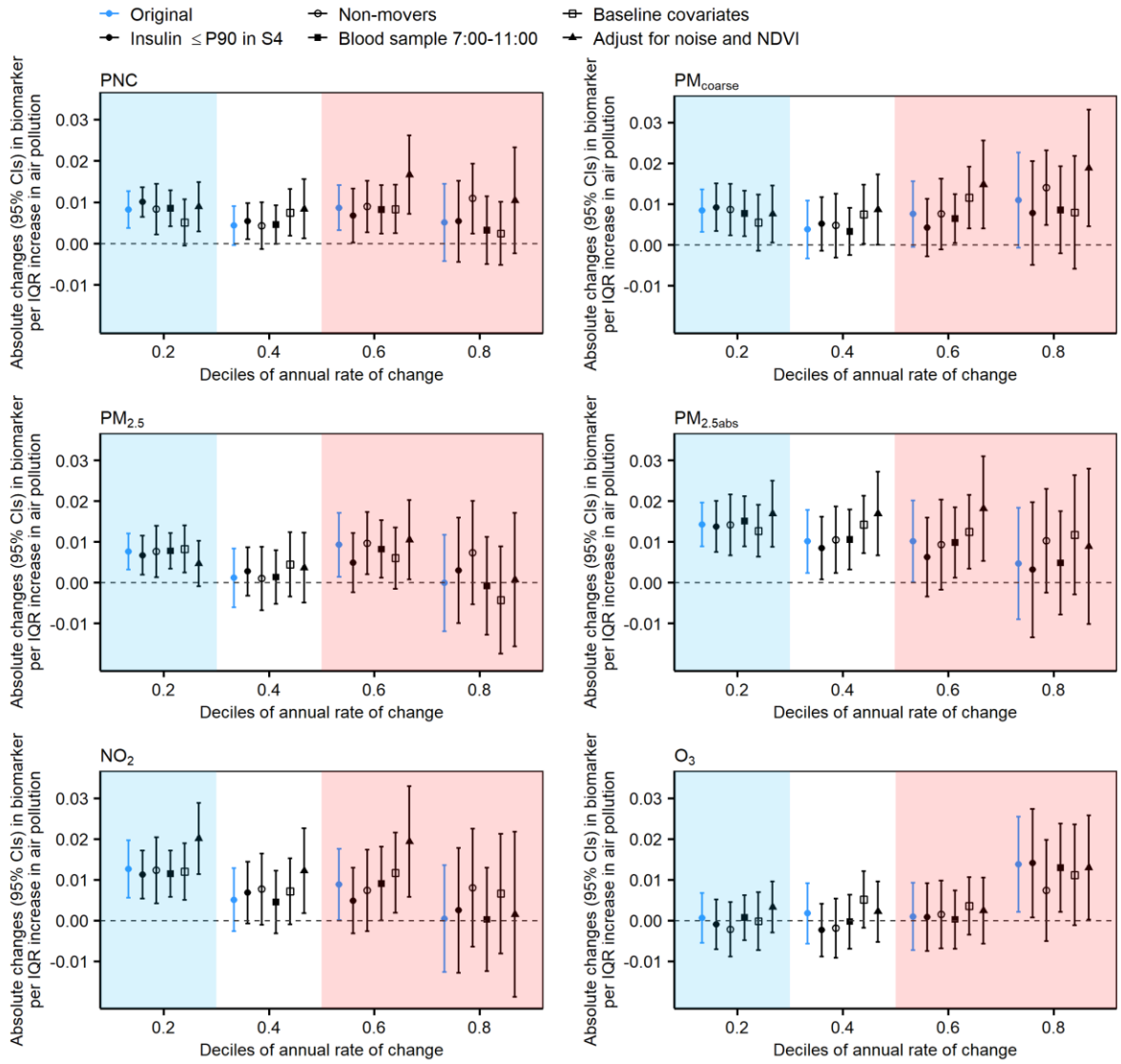

Figure S20. Absolute changes (95% CIs) in the annual rate of change in HOMA-IR per IQR increase in air pollutant concentrations in sensitivity analyses.

Original: main quantile regression model (number of observations remained in the analysis (*N*) = 2,242). Insulin ≤ P90 in S4: participants with fasting insulin concentrations ≤ the 90th percentile (21·9 µIU/ml) in KORA S4 (*N*=2,173). Non-movers: participants who did not move during S4 to FF4 (*N*=1,840). Blood sample 7:00-11:00: blood samples drawn between 7:00 AM and 11:00 AM (*N*=2,224). Baseline covariates: without adjustment for the annual rate of change in BMI and smoking pack-years (*N*=2,242). Adjust for noise and NDVI: with further adjustment for road traffic noise and NDVI in the main models (*N*=2,242). Blue shaded area on the left side indicates annual rate of change below zero; red shaded area on the right side indicates annual rate of change above zero; unshaded area in the middle indicates stable biomarker levels over years. An IQR increase was $2{\cdot}0\times10^{3}$/cm^3 for PNC, 1·4 µg/m^3 for PM_{coarse}, 1·4 µg/m^3 for $PM_{2{\cdot}5}$, $0{\cdot}3\times10^{-5}$/m for $PM_{2{\cdot}5abs}$, 7·1 µg/m^3 for NO_2, and 3·5 µg/m^3 for O_3.

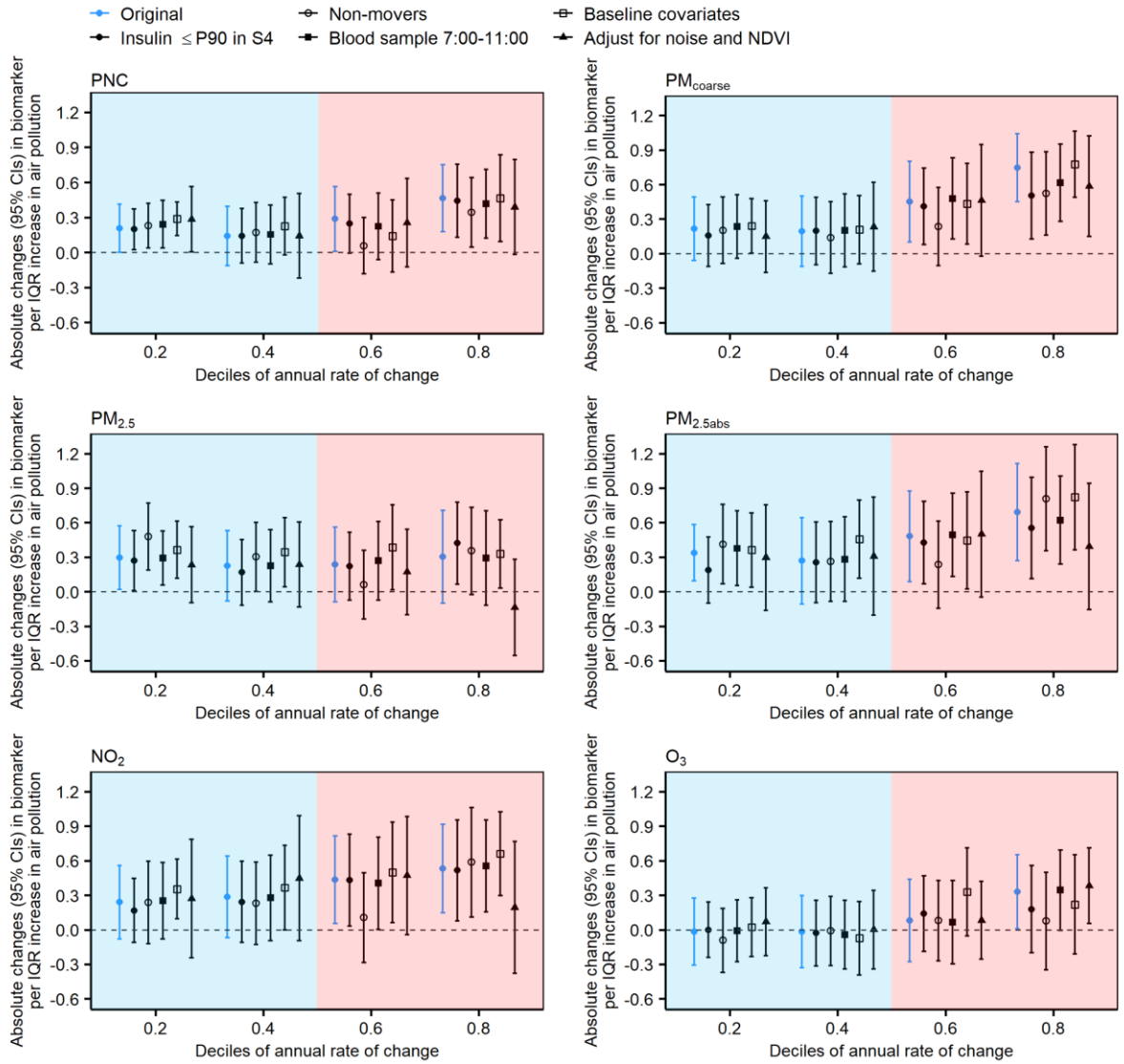

Figure S21. Absolute changes (95% CIs) in the annual rate of change in HOMA-B per IQR increase in air pollutant concentrations in sensitivity analyses.

Original: main quantile regression model (number of observations remained in the analysis (*N*) = 2,242). Insulin ≤ P90 in S4: participants with fasting insulin concentrations ≤ the 90th percentile (21·9 µIU/ml) in KORA S4 (*N*=2,173). Non-movers: participants who did not move during S4 to FF4 (*N*=1,840). Blood sample 7:00-11:00: blood samples drawn between 7:00 AM and 11:00 AM (*N*=2,224). Baseline covariates: without adjustment for the annual rate of change in BMI and smoking pack-years (*N*=2,242). Adjust for noise and NDVI: with further adjustment for road traffic noise and NDVI in the main models (*N*=2,242). Blue shaded area on the left side indicates annual rate of change below zero; red shaded area on the right side indicates annual rate of change above zero. An IQR increase was $2{\cdot}0\times10^{3}$/cm^3 for PNC, 1·4 µg/m^3 for PM_{coarse}, 1·4 µg/m^3 for $PM_{2·5}$, $0{\cdot}3\times10^{-5}$/m for $PM_{2·5abs}$, 7·1 µg/m^3 for NO_2, and 3·5 µg/m^3 for O_3.

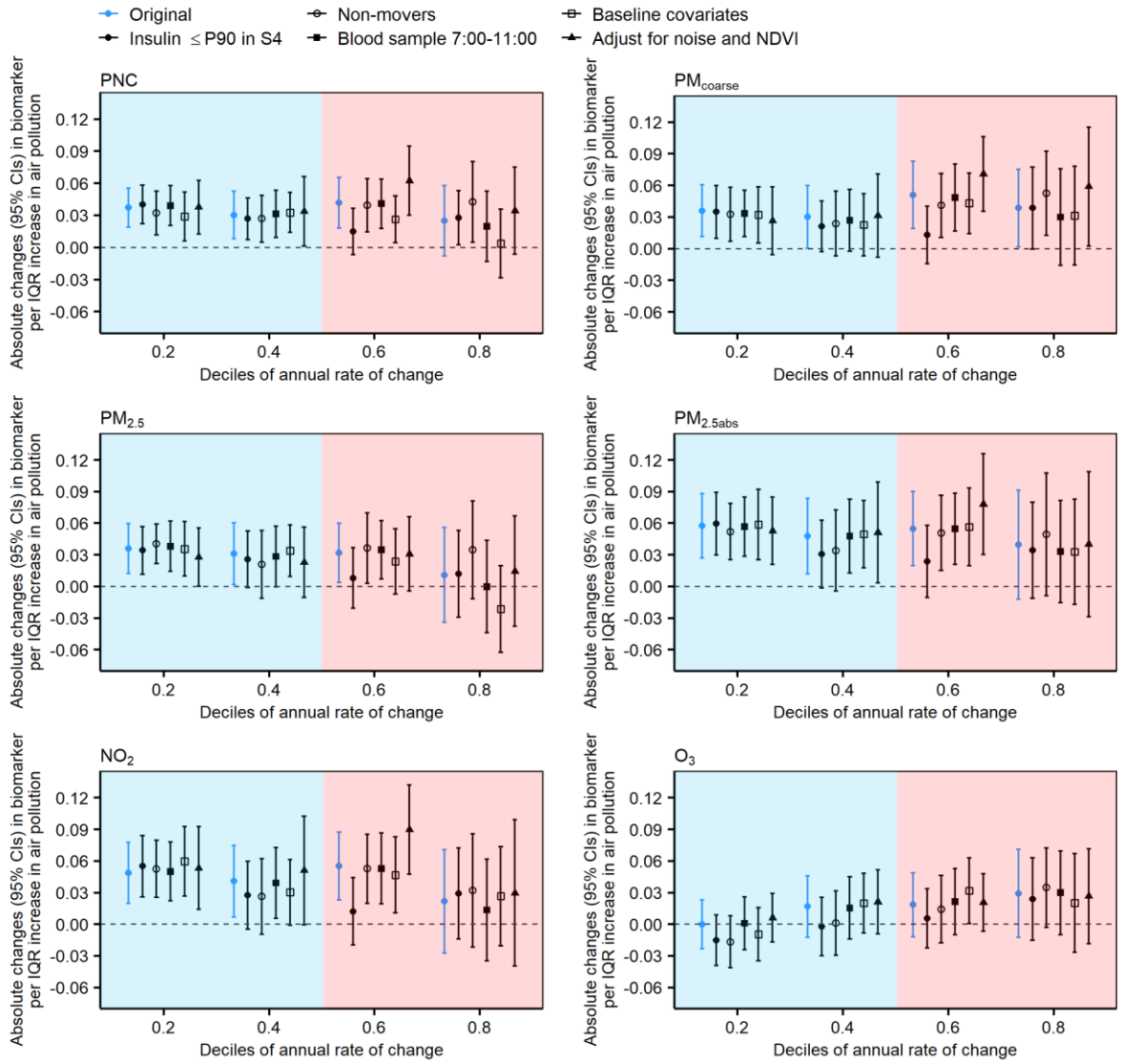

Figure S22. Absolute changes (95% CIs) in the annual rate of change in fasting insulin per IQR increase in air pollutant concentrations in sensitivity analyses.

Original: main quantile regression model (number of observations remained in the analysis (*N*) = 2,242). Insulin ≤ P90 in S4: participants with fasting insulin concentrations ≤ the 90th percentile (21·9 μIU/ml) in KORA S4 (*N*=2,173). Non-movers: participants who did not move during S4 to FF4 (*N*=1,840). Blood sample 7:00-11:00: blood samples drawn between 7:00 AM and 11:00 AM (*N*=2,224). Baseline covariates: without adjustment for the annual rate of change in BMI and smoking pack-years (*N*=2,242). Adjust for noise and NDVI: with further adjustment for road traffic noise and NDVI in the main models (*N*=2,242). Blue shaded area on the left side indicates annual rate of change below zero; red shaded area on the right side indicates annual rate of change above zero. An IQR increase was $2{\cdot}0\times10^{3}/cm^{3}$ for PNC, 1·4 $\mu g/m^{3}$ for PM_{coarse}, 1·4 $\mu g/m^{3}$ for $PM_{2{\cdot}5}$, $0{\cdot}3\times10^{-5}/m$ for $PM_{2{\cdot}5abs}$, 7·1 $\mu g/m^{3}$ for NO_2, and 3·5 $\mu g/m^{3}$ for O_3.

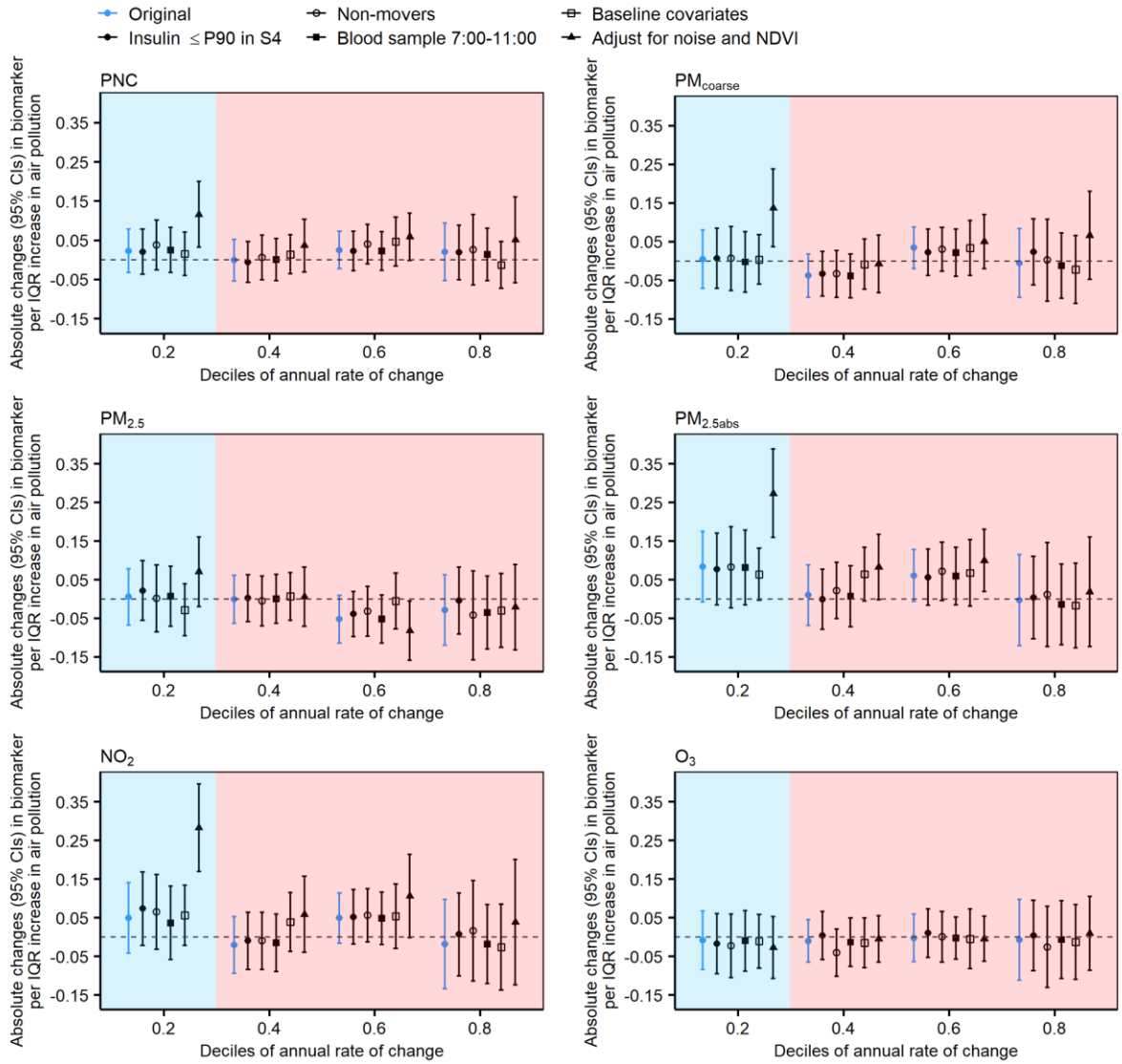

Figure S23. Absolute changes (95% CIs) in the annual rate of change in fasting glucose per IQR increase in air pollutant concentrations in sensitivity analyses.

Original: main quantile regression model (number of observations remained in the analysis (*N*) = 2,242). Insulin ≤ P90 in S4: participants with fasting insulin concentrations ≤ the 90th percentile (21·9 µIU/ml) in KORA S4 (*N*=2,173). Non-movers: participants who did not move during S4 to FF4 (*N*=1,840). Blood sample 7:00-11:00: blood samples drawn between 7:00 AM and 11:00 AM (*N*=2,224). Baseline covariates: without adjustment for the annual rate of change in BMI and smoking pack-years (*N*=2,242). Adjust for noise and NDVI: with further adjustment for road traffic noise and NDVI in the main models (*N*=2,242). Blue shaded area on the left side indicates annual rate of change below zero; red shaded area on the right side indicates annual rate of change above zero. An IQR increase was $2{\cdot}0\times10^{3}$/cm^3 for PNC, 1·4 µg/m^3 for PM_{coarse}, 1·4 µg/m^3 for $PM_{2{\cdot}5}$, $0{\cdot}3\times10^{-5}$/m for $PM_{2{\cdot}5abs}$, 7·1 µg/m^3 for NO_2, and 3·5 µg/m^3 for O_3.

References

1. Huth C, Beuerle S, Zierer A, et al. Biomarkers of iron metabolism are independently associated with impaired glucose metabolism and type 2 diabetes: the KORA F4 study. *Eur J Endocrinol* 2015; **173**(5): 643-53.
2. World Health Organization. Definition, Diagnosis and Classification of Diabetes Mellitus and its Complications. Part 1: Diagnosis and Classification of Diabetes Mellitus. *World Health Organization* 1999.
3. Hivert M-F, Sullivan L, Shrader P, et al. Insulin resistance influences the association of adiponectin levels with diabetes incidence in two population-based cohorts: the Cooperative Health Research in the Region of Augsburg (KORA) S4/F4 study and the Framingham Offspring Study. *Diabetologia* 2011; **54**(5): 1019-24.
4. Huth C, von Toerne C, Schederecker F, et al. Protein markers and risk of type 2 diabetes and prediabetes: a targeted proteomics approach in the KORA F4/FF4 study. *Eur J Epidemiol* 2019; **34**(4): 409-22.
5. Pitchika A, Hampel R, Wolf K, et al. Long-term associations of modeled and self-reported measures of exposure to air pollution and noise at residence on prevalent hypertension and blood pressure. *Sci Total Environ* 2017; **593-594**: 337-46.
6. Markevych I, Fuertes E, Tiesler CM, et al. Surrounding greenness and birth weight: results from the GINIplus and LISAplus birth cohorts in Munich. *Health & Place* 2014; **26**: 39-46.